Norwegian University of Life Sciences

Master's Thesis 2020 30 ECTS
Faculty of Bioscience

Simulation analysis of the impacts of climate change and scenarios of adapted cropping practices on the risk of brown rust development in winter wheat.

Gladys Adu Asieduwaa
Double degree Master of Science in Agroecology

This document was written by an ISARA and NMBU student in the framework of a convention with Institut national de la recherche agronomique (INRAE). For all citing, communication, or distribution related to this document, ISARA and NMBU must be mentioned.

Acknowledgment

I express my passionate appreciation to the Almighty God for His provisions, grace, and tender mercies towards me from the beginning of my master's degree and throughout this research. I am grateful to TERRA ISARA and Dr. Alexander Wezel (head of the committee, program coordinator, and my lecturer) for selecting and honouring me a scholarship to undertake this degree.

I am very appreciative of the OPERATE program for funding this research and to my external supervisor, Dr. Jean-Noël Aubertot, for selecting me for this project and for his persistent leadership, help, and criticism that made me more serious towards my research and to Dr. Camilo Corrales (post-doc) for his generous help with data mining. I am very grateful to my school supervisors; Prof. Tor Arvid Breland (NMBU) and Dr. Jean-Sébastien Beaulne (ISARA) for their encouragements, advices, and support throughout my research and not forgetting Dr. Aurélie Ferrer for the immense knowledge imparted to me during my second year at ISARA, which helped me throughout my research work.

Finally, honest thanks go to my siblings for their support, motivation, and encouragement throughout my degree and this research; I am grateful to you all. I thank God for my parents, without them I would not be here today and could not have done this without them, I love you both.

Abstract

The challenge of climate change in agriculture is a global threat and to meet the demand for food of future generations and ensure global food security, there is a great need to use agroecological measures to reduce or eliminate this threat. Wheat, both a staple crop and an export crop in France, is not an exception to suffering the negative impacts of climate change. This research aimed at simulating the impacts of climate change on brown rust development in wheat. In order to do so, the information on brown rust severity embedded within warning bulletins combined with weather data of twenty regions from 1986–2010 was used to create a simple classifier to predict brown rust severity on wheat. The machine learning tool WEKA was used to create a simple J48 (C4.5) pruned decision tree model using the data of the warning bulletins and the Safran weather database (8 km * 8 km grid, Météo France). Temperatures above 15 °C were found to increase the severity of brown rust. Relative humidity between 70% and 90% were also predicted to affect brown rust development. For the simulation study, the risk of brown rust was quantified under climate change and an adaptation scenario that consisted of using mulch of pea residues for the 150 years using the dynamic model, STICS MILA. These simulated brown rust severity data were then used as input variables in the WHEATPEST model, to calculate the yield losses caused by the disease. Also, RUE values increased as temperature increased, and it was predicted that over the 150 years, temperature, RUE, and brown rust severity would continue to increase. Yield is predicted to be impacted either negatively or positively by climate change as in some cases, high temperature resulted in increased yield. For the decision tree model, the training set test option had a high performance as described by the ROC Area value of 0.974 whereas, in the cross-validation test option, the ROC Area value of 0.647 was recorded. Brown rust was predicted to cause yield losses for the simulated years and adapting agroecological cropping practices would be beneficial in suppressing these losses.

Keywords: *Triticum aestivum*, *Puccinia triticina*, modelling, warning bulletins

Table of Contents

List of Figures

List of Tables

List of abbreviations/acronyms

Arvalis- the French Arable Crops, Research and Development Institute

cumraint(n) – cumulative intercepted radiation of current day (MJ m^{-2})

cumraint(n-1) – cumulative intercepted radiation of previous day (MJ m^{-2})

cumrg – cumulative global radiation (MJ m^{-2})

masec(n) – aboveground biomass of current day ($t.ha^{-1}$)

masec(n-1) – aboveground biomass of previous day ($t.ha^{-1}$)

Mon_MUP – adaptation cropping practice of using mulch with pea residues for the location, Mons

RH- relative humidity (%)

RUE – Radiation Use Efficiency (%)

temp- temperature

tmax – maximum temperature (°C)

tmin – minimum temperature (°C)

1. CHAPTER 1: INTRODUCTION

1.1. Context and problem statement of the study

The agri-food system is progressively under pressure due to several challenges (Hubeau et al., 2017). Among such challenges, adaptation to climate change is a priority. Lower agricultural production caused by climate change would strongly impact the food system. In order to eliminate the defect in the agri-food system to meet the needs of the growing population, there is a need to ensure the sustainability of the food system (Francis et al., 2003). According to Béné et al. (2019), this increasing concern in food systems is a result of multiple challenges that range from ecological, equity and resources, trade, issues of diet, and health. It encompasses the understanding that feeding the population today and, in the future, involves more than just a 'more-food' approach and that extra emphasis needs to be placed on diet quality and safety, the ecosystem 'foodprint', and socio-economic imprints of supply chains (Béné et al., 2019). A bigger concern arose in recent years when specialists realized that making food systems more sustainable and nutrition-reactive is not sufficient to address the issue of malnutrition. Hence, more attention needs to be paid to the governance and stakeholders of the food systems in the populated world (Tschirley et al., 2013).

Several challenges are encountered in the transformation of agri-food systems toward sustainability. These challenges can span from ecological, economic, and social perspectives at relevant levels in space and time. Anthropogenic greenhouse gas emissions are altering the climatic conditions in the world and this is likely to result in rising temperatures, shifts in rainfall patterns, and higher rates of weather extremities (IPCC, 2009). An ecological and social perspective of the impacts of climate change is the awareness and assessment of the effects of climate change on crop diseases that are becoming a priority in the sense of climate change and food safety issues (Lamichhane et al., 2015). Biodiversity conservation is not only essential to our environment, but it is also a critical prerequisite for safe, sustainable food systems. For more diverse, healthier, and more balanced nutrition and more resilient food systems, there is a need for sustainable diversified cropping and enhanced genetic qualities of crops (FAO, 2019). From an economic perspective, one challenge is access to funds to invest in agricultural production. When these funds are made available, they can efficiently and concisely help solve a variety of problems such as conserving the environment, reducing hunger and poverty through the development of a sustainable food system, as well as tackling climate change (FAO, 2019).

Due to the need for the understanding of such challenges to eliminate or reduce the negative impacts of climate change on agricultural production, several agricultural research and development actors have together come up with a research program named OPERATE (crOP disEase Response to climATE change adaptation), under the umbrella of the [INRAE ACCAF metaprogram](). The OPERATE project aims to quantify the impacts of climate change and farmers' adaptation scenarios for three arable crops (sunflower, potato, and wheat).

Wheat is an important cereal grain in France, which is the biggest producer in Europe (Oishmaya, 2019). As of 2015, wheat accounted for 54% of French cereals and occupied about 4 million hectares (Ministère de l'Agriculture et de l'Alimentation, 2015). The greatest production is done in the north of the country and winter wheat is the main type produced. Wheat is usually sown in the autumn season and harvested in August of the following year. In Europe, several diseases such as rusts and blotches cause yield and quality losses yearly with the most common control method being the application of fungicides (Curtis, 1992). At the end of the 20th century, brown rust was considered the most damaging foliar diseases on wheat in Europe (Goyeau & Lannou, 2011; Dean et al., 2012; Kolmer, 2013). This disease caused by *Puccinia triticina* is characterised by brownish-orange and usually, circular spots are known as uredinia that appear on the upper surface of leaves (Robin et al., 2018) and is found in most regions in France where wheat is grown. The main host is usually wheat and the alternate host is the meadow rue (Bolton et al., 2008). In France, the alternative host, *Thalictrum speciosissimum*, is not present and is very rare in Europe (Azzimonti, 2012). Brown rust is documented as a prevalent pathogen in wheat production areas where it causes substantial yield losses (Roelfs, 1992; Kolmer, 2005). In wheat, 60-70% infection on the leaf during the emergence of the spike can lead to 30% of yield losses (Huerta-Espino et al., 2011).

Lopes et al. (2018), confirm that sporadic weather conditions associated with rising temperatures and rainfall cause specific challenges for wheat producers, and such patterns can also decrease improvements in the genetics of winter wheat. Several studies showed the link between climate variability and wheat production. The CIMMYT, in 2017, reported that temperature increases as a result of climate change will cause a 20-30% decline in wheat production in developing countries. According to Gouache et al. (2012), several studies in France show a negative relationship between rising temperatures and crop yields for wheat, maize, and barley (Lobell et al., 2011). The optimum conditions for the development of brown rust are dewy environments, mild temperatures (15-25°C) usually during the flowering phase of hosts (Kolmer, 2017).

The research conducted during the internship focused on the analysis of the effects of climate change and adaptation scenarios of cropping practices on brown rust development. To simulate the impact of climate change on the development of brown rust in winter wheat, a thorough reading of the literature on climate change, brown rust, and the 2 hard-system modelling approach used;

WHEATPEST and STICS-MILA, and the protocols needed to carry out simulations was done. The articles used were derived from web of science, google scholar, and some articles from my external supervisor. The dynamic model STICS MILA (Caubel et al., 2012) was used to quantify the risk of brown rust under climate change and the adaption scenario of the use of mulch with pea residues. These simulations of brown rust severities were run in the WHEATPEST model (Willocquet et al., 2008) to calculate yield losses caused by brown rust.

The following research questions were addressed:

i. Does climate change promote the epidemics of Puccinia triticina responsible for brown rust on winter wheat in the regions documented?
ii. How can cropping practices be adapted to control the development of the disease?
iii. What is the risk of this biotic stress on winter wheat and can we quantify the associated damages?

1.2. Delimitations of the study

This study only elaborated on the impact of climate change on wheat production with a focus on only one disease (brown rust). A comprehensive review describing the state of the art can be found in appendix I.

2. CHAPTER 2: RESEARCH METHODOLOGY

This research was in two main parts; 1. the warning bulletins and 2. the simulation study.

2.1. Part 2: Warning bulletins

To forecast the severity of disease over years, weather data from the SAFRAN database of Météo-France, provided by the Agroclim unit and severity data from warning bulletins were used. The acquired data files were for the years 1982 to 2010 (depending on the available data for each region). A total of twenty regions (Alsace, Aquitaine, Auvergne, Basse-Normandie, Bourgogne, Bretagne, Center-Val de Loire, Champagne-Ardenne, Franche-Comté, Haute-Normandie, Île-de-France, Languedoc-Roussillon, Limousin, Lorraine, Midi-Pyrénées, Nord-Pas de Calais, Pays de la Loire, Picardie, Poitou-Charentes and Provence-Alpes Côte d'Azur) were covered.

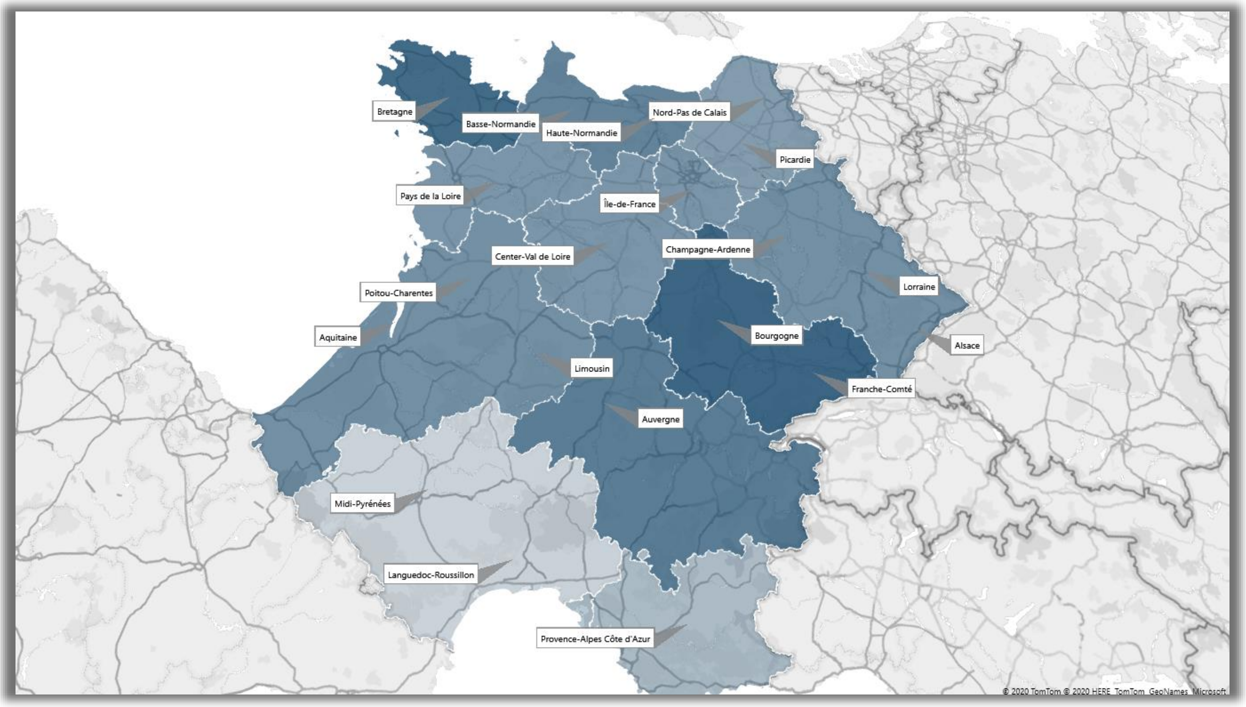

Figure 1: Map of France showing the 20 regions for which warning bulletins were covered from 1982–2010.

The data provided included several indicators of weather and the brown rust severity data documented for these regions over the years. The weather data consisted of varying indicators for the following weather conditions; temperature, relative humidity, global radiation, and rainfall. For each weather variable, data was taken for each trimester in each year (January–March (t1), April–June (t2), July–September (t3), and October–December (t4)); (see appendix V).

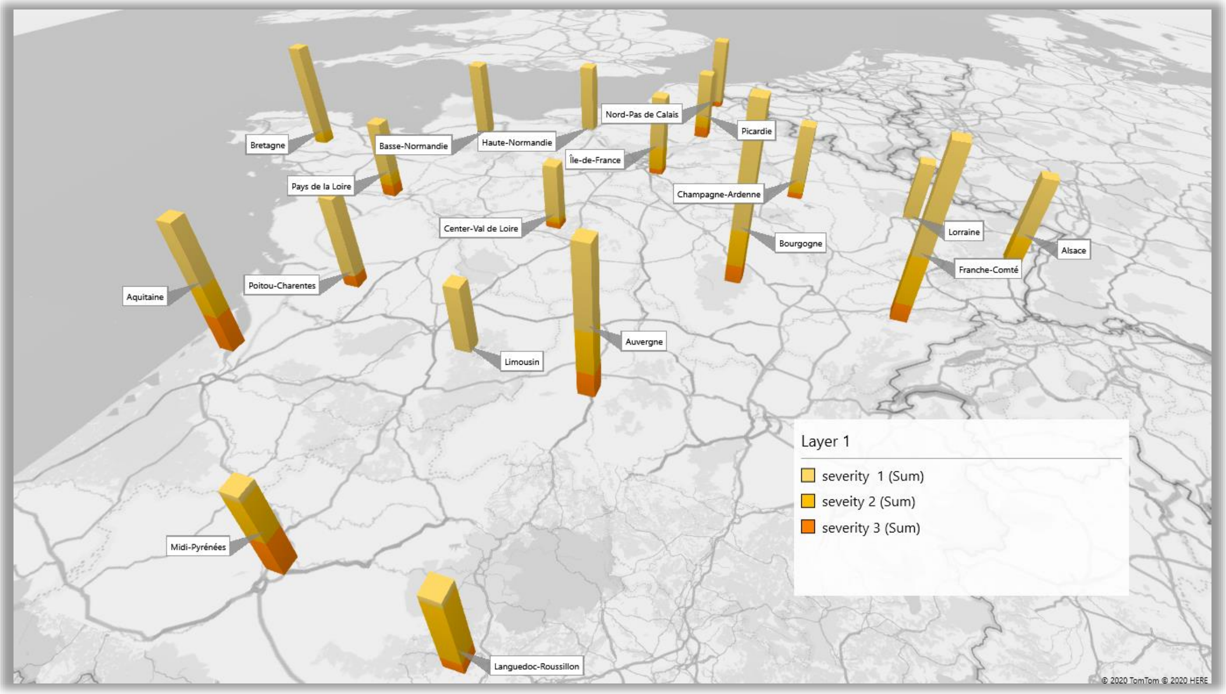

Figure 2: A map of the 20 regions documented with their cumulated distributions of BRS. Severity 1= low, severity 2= intermediate and severity 3= high.

2.1.1. Collation of warning bulletins data files

For each scenario, that is, a region per year, the brown rust severity data was bulleted by collecting the corresponding brown rust severity and inputting them into excel. For recording the warning bulletins, the selected range was 1–3, where 1 is low, 2–intermediate, and 3–high. Aside from the bulletin for the severity of the disease, a detailed remark and justification for the particular bulletin for each scenario were added. See appendix II for an example of the raw excel datasheet. The weather data consisting of varying indicators were all placed in one excel sheet with their corresponding collated region per year per severity data (appendix III).

2.1.2. Processing of warning bulletins data files

After gathering the needed warning bulletin data, the open-source data mining machine learning tool, Weka, was used to process and analyse the data. This tool was used to create a simple model for the bulletin of brown rust severity. The dependent variable used to create this model was the severity of the disease whereas the independent variables were the varying indicators for the selected climatic conditions. The j48 classifier, a C4.5 decision tree, was used to produce a simple pruned tree model. Two approaches were conducted: a training set and cross-validation at 10 folds. For more information on the C4.5 decision tree, see Ross Quinlan (1993) and detailed information on WEKA can be found by Eibe et al. (2016).

2.2. Simulation Study

2.2.1. Data retrieval

Data processed using the STICS-MILA model to acquire input variables needed to run simulations on WHEATPEST (disease inoculum data, and climatic data and scenarios– daily records of rainfall, maximum temperature, minimum temperature, solar radiation, and other input variables), was provided by Arvalis for the location Mons. These data files comprised of weather data and scenarios, crop data, and inoculum data for the cropping adaptation scenario of "Mon_MUP" from the year 1951 to 2100. The inoculum data used was 10000 inoculums (the intensity of simulated rust pathogen released to stimulate the development of the disease). The management practices for Mon_MUP were cultivation using mulch with pea residues at an early sowing date of 24th September, no-tillage, and an available water storage capacity (RU) value of 200 mm.

Table 1: Variables used for the simulation in the WHEATPEST model, the state variables of WHEATPEST, and the output variable derived from WHEATPEST and their units.

Input variables	**State variables**	**Output variable**
Maximum temperature (°C)	Leaf Biomass (g m^{-2})	Simulated yield (g m^{-2})
Minimum temperature (°C)	Steam Biomass (g m^{-2})	
Radiation Use Efficiency (g MJ^{-1})	Ear Biomass (g m^{-2})	
Brown rust severity (% leaf surface)	Root Biomass (g m^{-2})	

2.2.2. Calculations

2.2.2.1 RUE

After receiving the large data files simulated by STICS-MILA, to ease the complexity and aid the use of these data, the files were split into the various years (from 1950-2100) using R studio. The daily RUE values for each weather scenario and crop data were calculated using the R script presented in appendix VI. For each year, using the ratio between the daily increase of aboveground biomass divided by the Intercepted Photosynthetic Active Radiation increase as described by Tripathi et al. (2018) and Mariscal et al. (2000). After the calculation, in order to get the correct units for the calculated values, the values were multiplied by 100 g.

Rue was calculated as:

$$RUE = \frac{[\mathrm{masec(n)} - \mathrm{masec(n-1)}]}{[\mathrm{cumraint(n)} - \mathrm{cumraint(n-1)}]}$$

where,

masec(n)= aboveground biomass of current day ($t.ha^{-1}$)

masec(n-1)= aboveground biomass of previous day ($t.ha^{-1}$)

cumraint(n)= cumulative intercepted radiation of current day ($MJ\ m^{-2}$)

cumraint(n-1)= cumulative intercepted radiation of previous day ($MJ\ m^{-2}$)

2.2.2.2 Temporal Integration of RUE

Due to the need for an indicator to summarize RUE during the cropping seasons over the 150 years, RUE was integrated over time using the following formula:

$$Temporal\ Integration\ of\ RUE = \sum_{i=1}^{n-1} \left(\frac{x_i + x_{i-1}}{2}\right)(t_{i+1} - t_i)$$

where,

xi= the temporal integration of RUE of the previous day

xi+1= the temporal integration of RUE of the current day

ti= the previous day

ti+1= the current day

n= number of observations

2.2.2.3 Area Under Disease Progress Curve (AUDPC)

The disease severity recorded on a daily basis for the 150 years were used to produce the AUDPC using the following formula as proposed by CIMMYT (Jeger et al., 2001):

$$AUDPC = \sum_{i=1}^{n-1} \left(\frac{x_i + x_{i-1}}{2}\right)(t_{i+1} - t_i)$$

where,

xi= the rust severity of the previous day

xi+1= the rust severity of the current day

ti= the previous day

ti+1= the current day

n= number of observations

2.2.2.4 Thermal time

Yearly values of thermal time (º C day) were calculated using the formula proposed by Willocquet et al. (2008):

$$\mathrm{DTEMP} = \max\left(0, \left(\frac{tmax + tmin}{2}\right) - Tbase\right)$$

where,

DTEMP= daily increase in thermal time

tmax= maximum temperature

tmin= minimum temperature

Tbase = 0 °C

2.2.2.5 Yield estimation

The yield was calculated using the simulated biomass of leaf, stem, and ear in WHEATPEST using the simulated weather data from STICS-MILA and the above-ground biomass values from STICS-MILA. 85% of ear biomass was used and the formula used was:

$$yield\ simulated = \left[\frac{85\%\ (EarBM)}{sum\ of\ LeafBM, StemBM\ and\ 85\%\ (EarBM)}\right] * masec(n)$$

where,

EarBM= ear biomass

LeafBM= leaf biomass

StemBM = stem biomass

masec(n)= aboveground biomass

This formula and the use of the combination of datasets from both WHEATPEST and STICS-MILA used was because the dataset simulated with STICS-MILA did not include ear, leaf, and stem biomass but only above-ground biomass. WHEATPEST was then used to simulate these biomasses to simulate yield.

2.2.3. Data splitting and data organization

After the RUE calculation, the weather scenarios, the inoculum, and crop characteristics data files were organised. For each weather scenario, their corresponding inoculum data were matched to get the accurate and needed data for the simulation analyses. The organisation was done by computing each weather scenario data, their corresponding RUE data as well as their corresponding disease severity data. These three categories (weather data, RUE data, and disease severity data) were then used for the simulation.

2.2.4. Models and their operations

2.2.4.1 STICS-MILA

STICS-MILA is a suitable tool to identify and assess the role of various effects on disease pressure. STICS simulates crop operation at a daily time step at field level for an average plant, with input variables (climate, soil, and the crop system) while MILA simulates continuous epidemiological cycles at the crop level. STICS-MILA is a mechanistic, process-based, dynamic model that predicts significant variations in disease intensity between climatic periods and between scenarios (Caubel et al., 2017). Although it is complicated, it helps explain the evolution of disease development and simulate complex interactions. A detailed description of STICS-MILA is provided by Caubel et al. (2017).

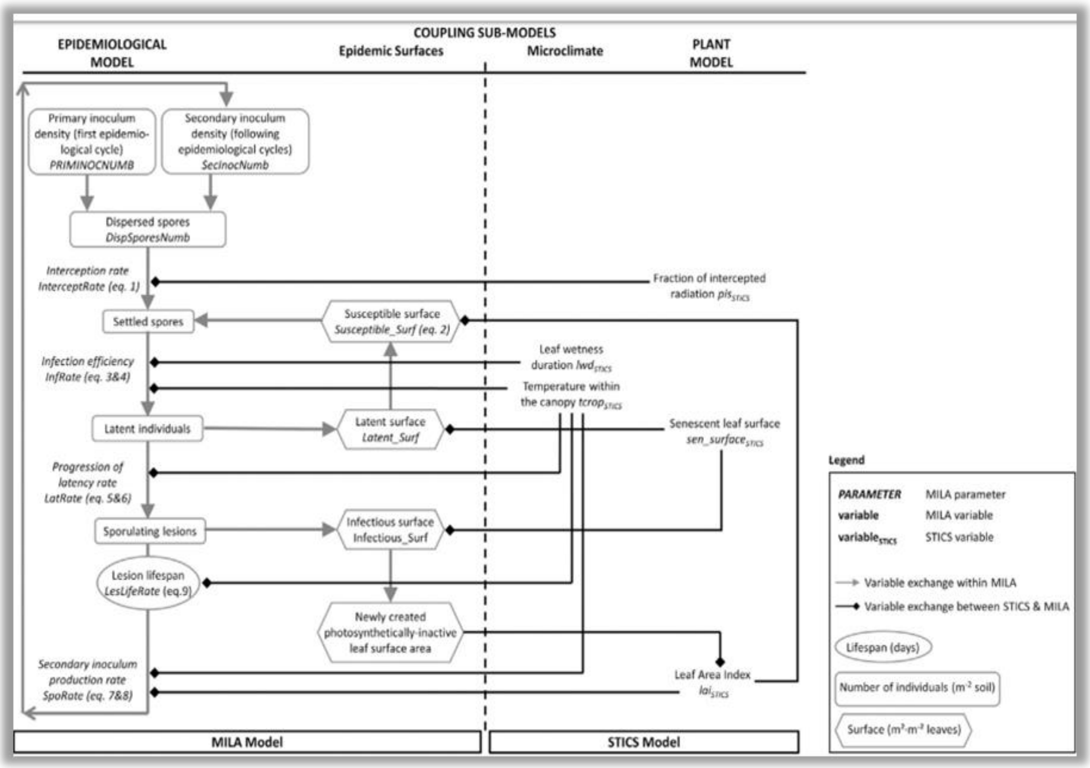

Figure 3: STICS coupled with MILA daily calculations and exchange variables (Caubel et al., 2017).

2.2.4.2 WHEATPEST

WHEATPEST (Willocquet et al. 2008) is a simple winter wheat crop model based on the physiological structure of plants (agro-physiological mode) that integrates damage mechanisms caused by multiple pests (pathogens, insects, weeds) and simulates the physiological effects of these pests on plant growth and yield. It considers the impacts of harmful organisms; it takes into 13 pests. WHEATPEST was implemented under Model Builder, a free web-based online modelling platform that is used to create and share dynamic models of diverse scientific fields (Aubertot et al, 2015). Model builder is user friendly and helps develop, edit, use and share models (https://xpest.inra.fr). Further details on WHEATPEST can be seen in Willocquet et al. (2008).

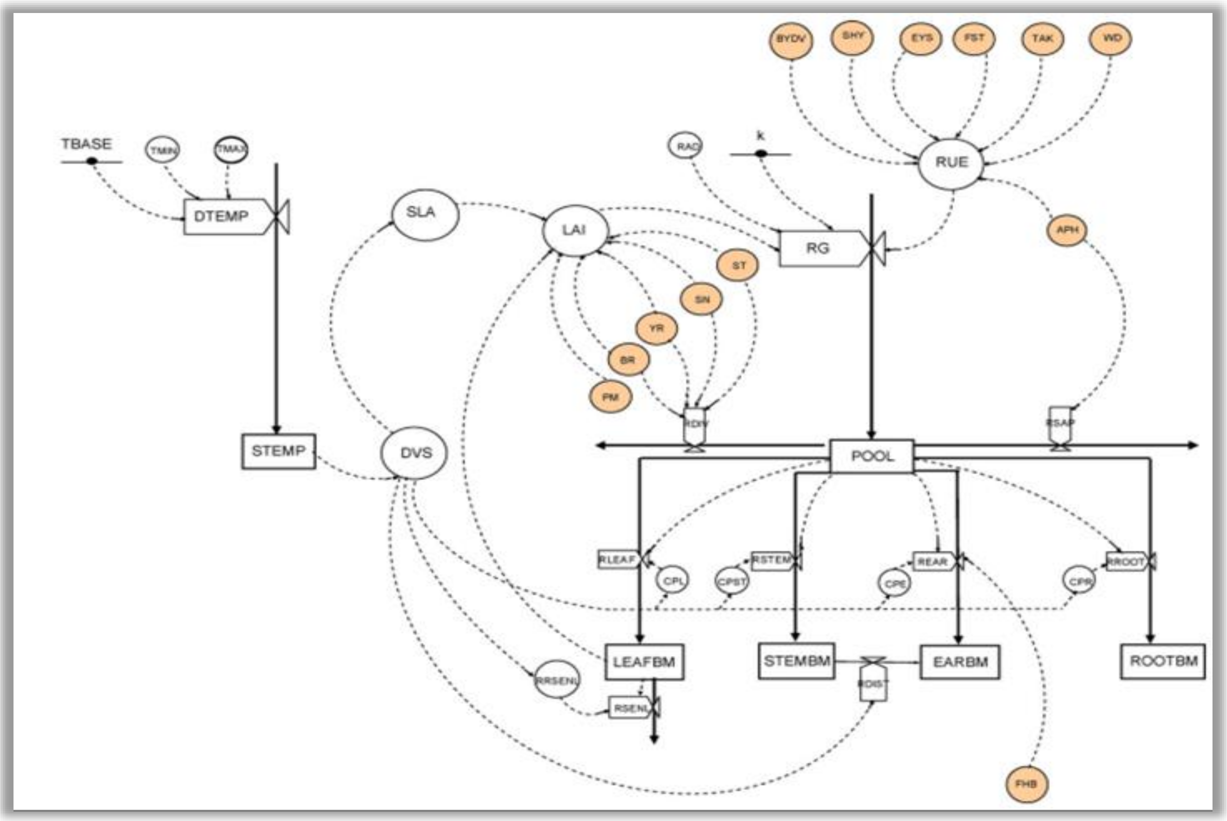

Figure 4: A simplified structure of the WHEATPEST model (Willocquet et al., 2008).

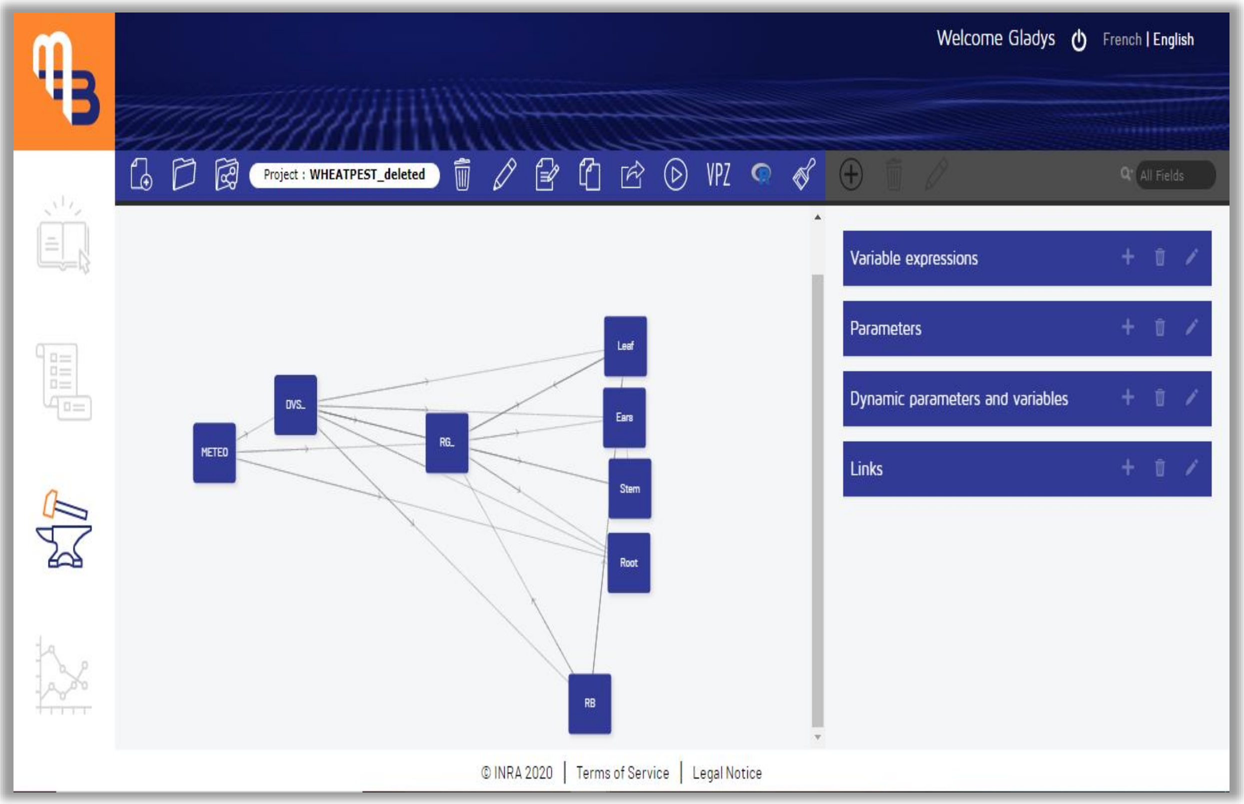

Figure 5: The interface of the WHEATPEST model used in ModelBuilder (https://xpest.inra.fr).

2.2.5. Modelling analysis

The analysis was done after all data had been computed and organised. The three categories of data organised (weather data, RUE data, and disease severity data) were then used for the simulation test. The model was evaluated by comparing the simulated output of the model with the observed data set.

3. CHAPTER 3: RESULTS

3.1. Warning bulletins

3.1.1. Analysis of data for region per year

In total, for the twenty regions, there were three hundred and four (304) instances of which Franche-Comté had the highest documented years as seen in figure 6. The region with the least logged years was Provence-Alpes Côte d'Azur. The range of years with the highest available data for all regions was between 2004–2006 (figure 7).

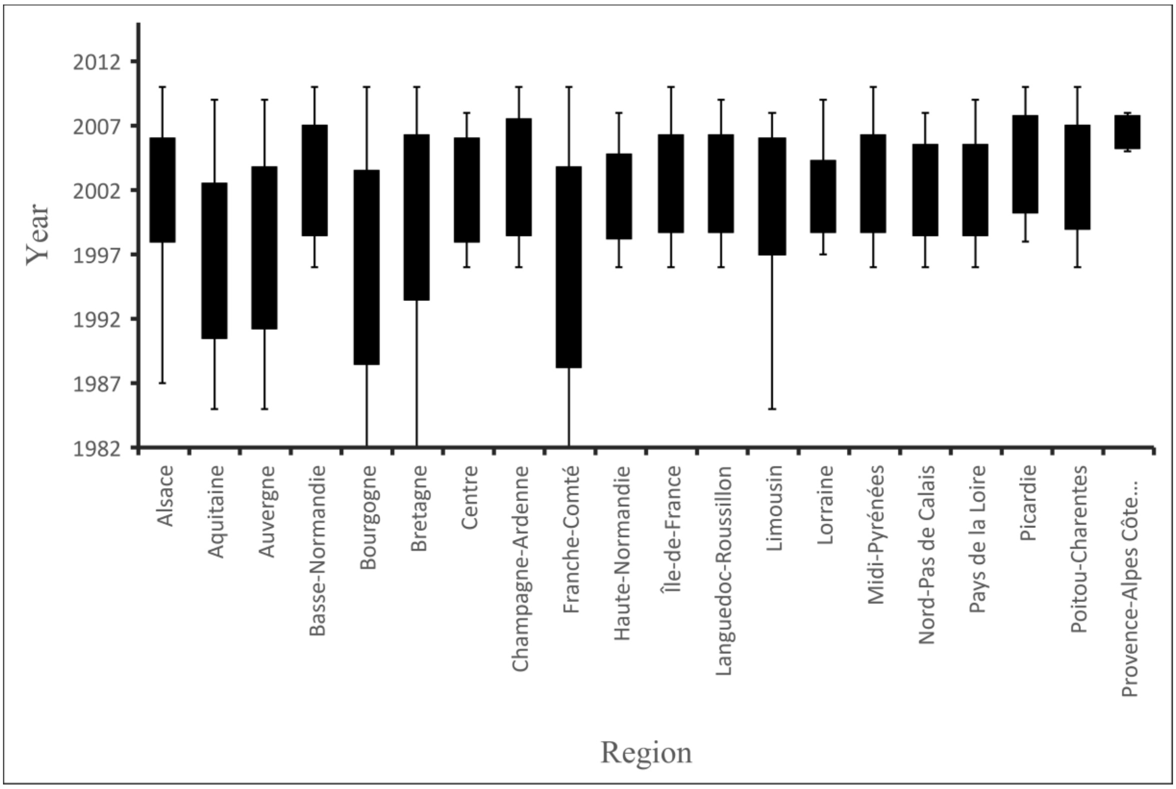

Figure 6: Documented warning bulletins over the years per region.

The lines indicate the range of years for each region and the black boxes show the distribution.

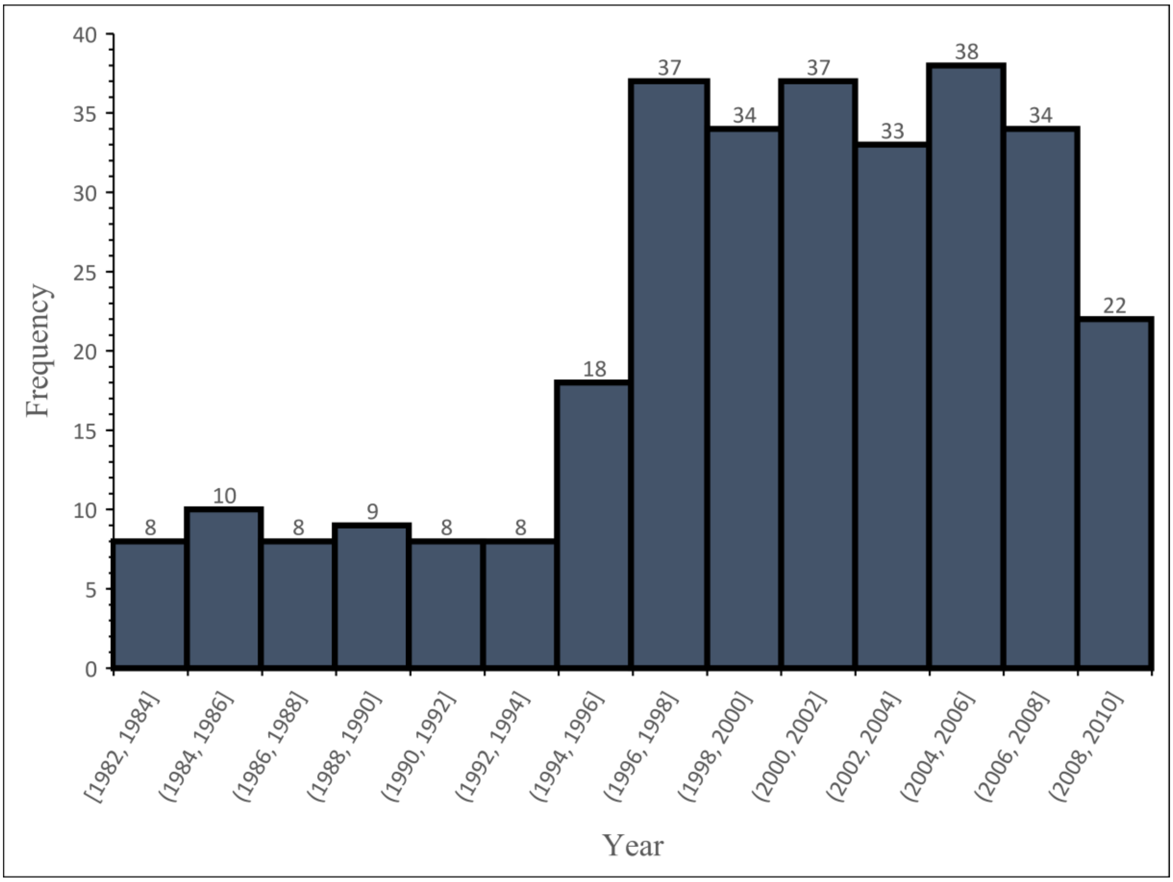

Figure 7: The frequency at which warning bulletins were documented for each year from 1982–2010.

3.1.2. The severity of brown rust documented

The brown rust severity for the documented years was mainly low at a frequency of 207. Only thirty-five (35) instances recorded a high severity of brown rust whereas intermediate cases were sixty-two (62) as seen in figure 8. In figure 9, it can be seen that of all instances of high severity of brown rust, the highest frequency was 6 and was recorded in the regions Aquitaine and Midi-Pyrénées whereas Bourgogne recorded the highest number of low cases at a frequency of 20. In all regions for all years, the most number of high brown rust severity cases at a frequency of 11 was recorded in 2007 while the highest number of low brown rust severity cases at a frequency of 16 was documented in the years 1997, 2003, and 2006 (figure 10).

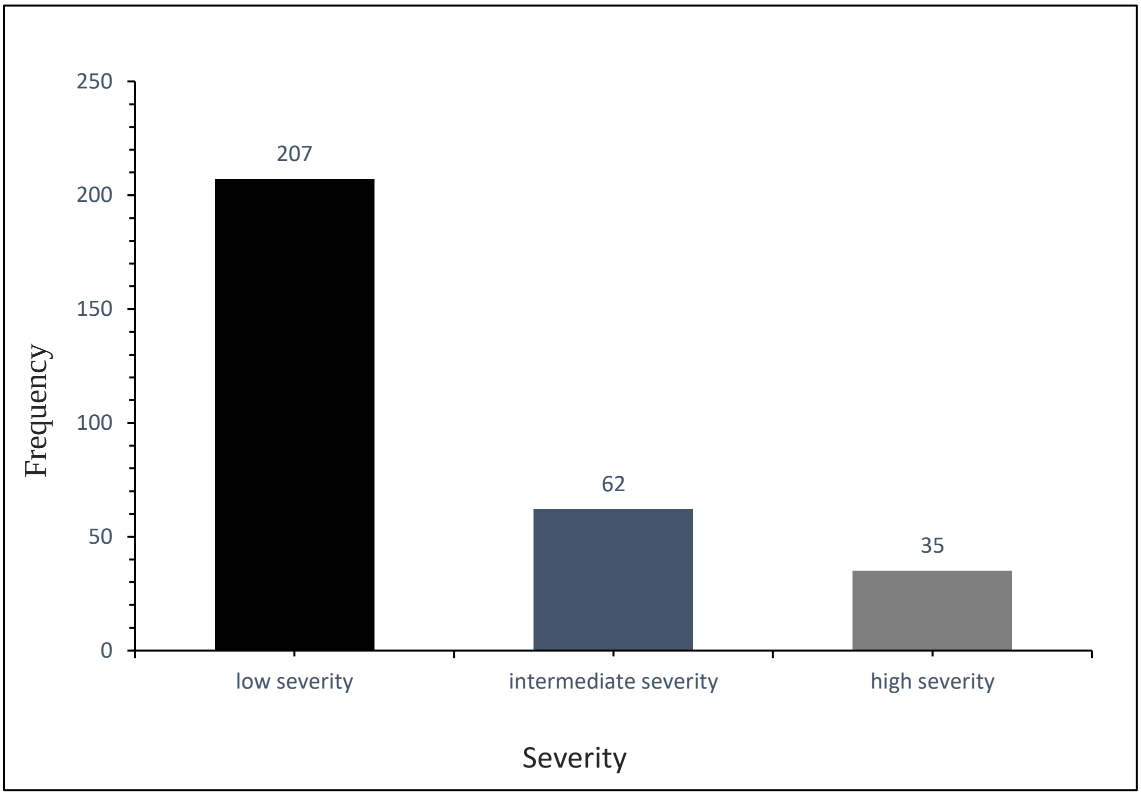

Figure 8: The frequency of brown rust severity for 1, 2, and 3: 1–low, 2–intermediate, and 3–high from 1982–2010 for the twenty regions.

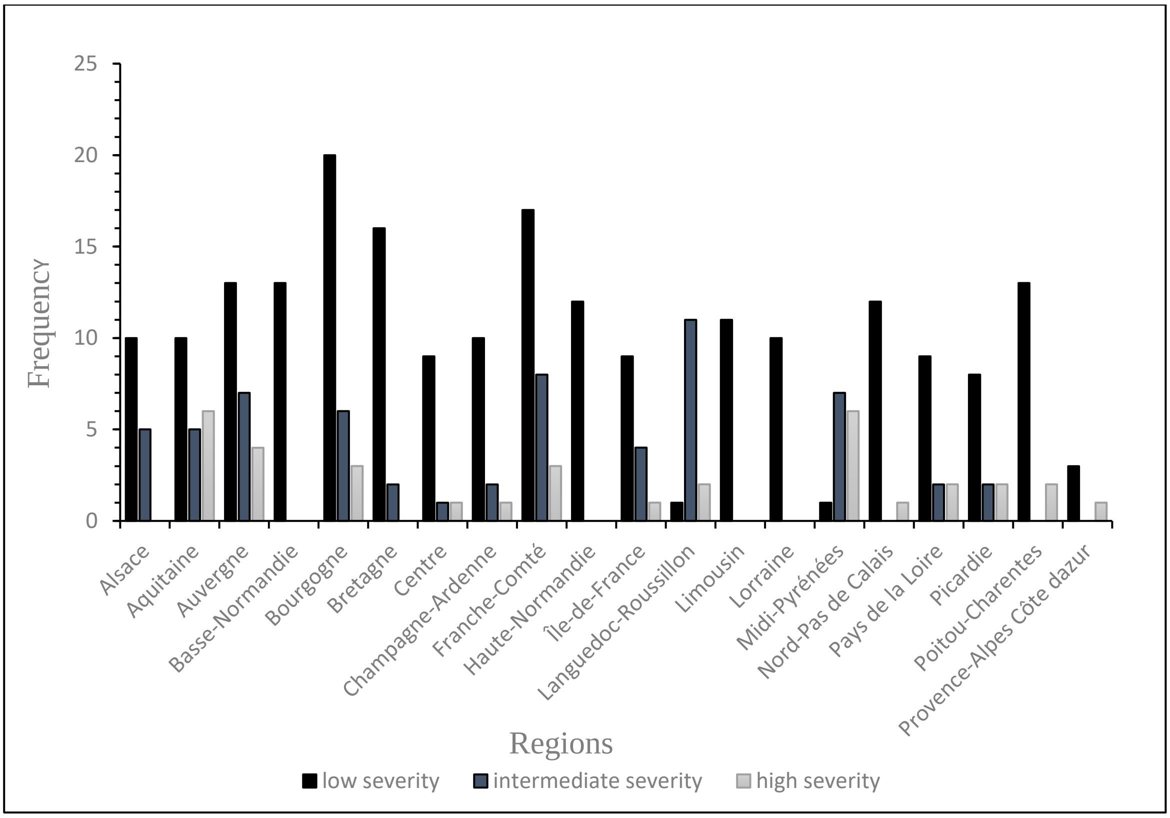

Figure 9: The frequency of brown rust severity per region from 1982–2010 for the twenty regions.

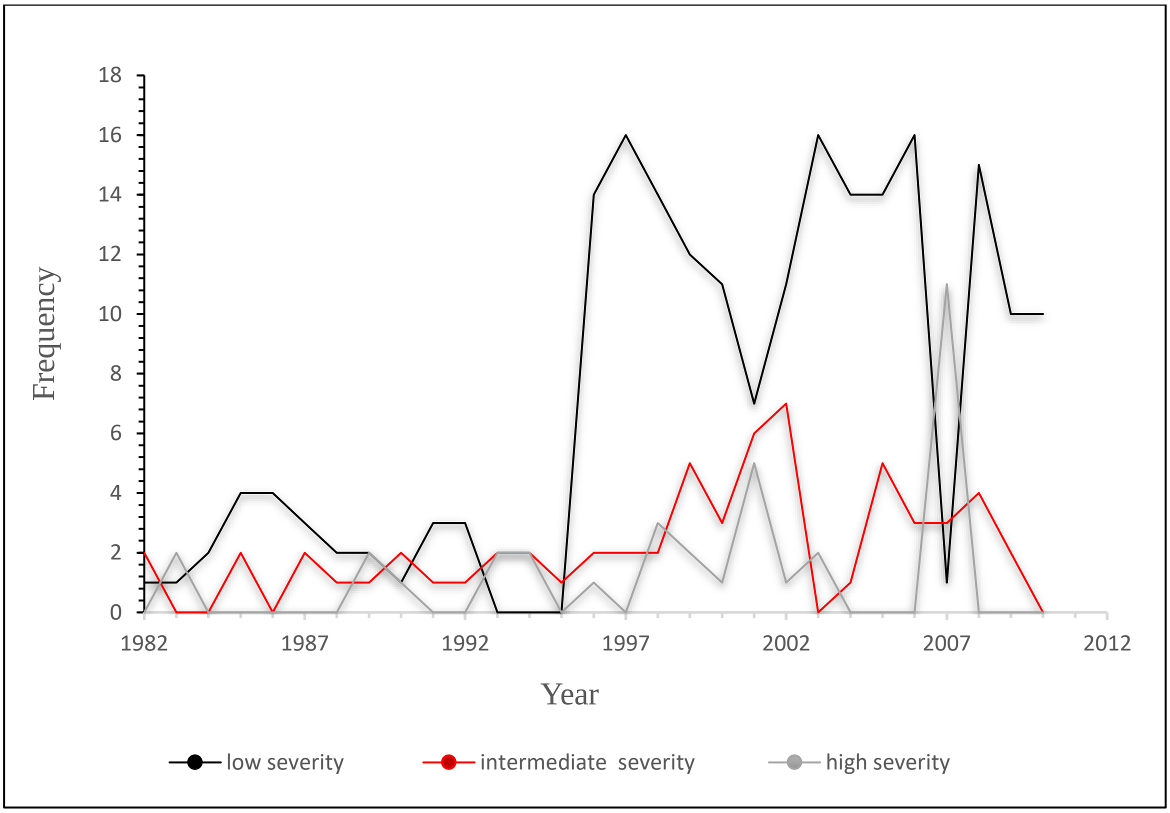

Figure 10: The frequency of brown rust severity per year from 1982–2010 for the twenty regions.

3.1.3. Decision tree (effects of varying climate indicators on BRS)

For the model, the number of instances (total number of cases) was three hundred and four (304) with one hundred and nine (109) potential explaining variables. The dependent variable being the rust severity and the independent variable being the 108 weather-based indicators. The tree has thirty-four (34) leaf nodes and the total number of nodes (tree size) is sixty-seven (67). In figure 11, it is observed that the first split is on V63 (med,tp,ther5,t1– median of the thermal time (5°C) during t1) which is supported by V81 (med,moy,tn,t3– median of daily average minimum temperatures in t3) and V77 (med,j,tx,sup32,t3– median of the number of days with tmax above 32°C in t3) if V63= 278.8 whereas the second split on V77 and V81 are supported by V69 (med,j,tx,sup25,t3– median of the number of days with tmax above 25°C in t3), V48 (med,sin,tm5<25,t2– median of the temporal integration during t2 of the sin2 function (0 when temp is below 5°C or above), and V86 (med,tn,t4– median of minimum temperatures in t4). Hence, V63, V81, and V77 are the most significant to differentiate among classes. Of all 108 attributes, only twenty-six (26) were captured and segregated among classes. See appendix V for the meanings of each variable.

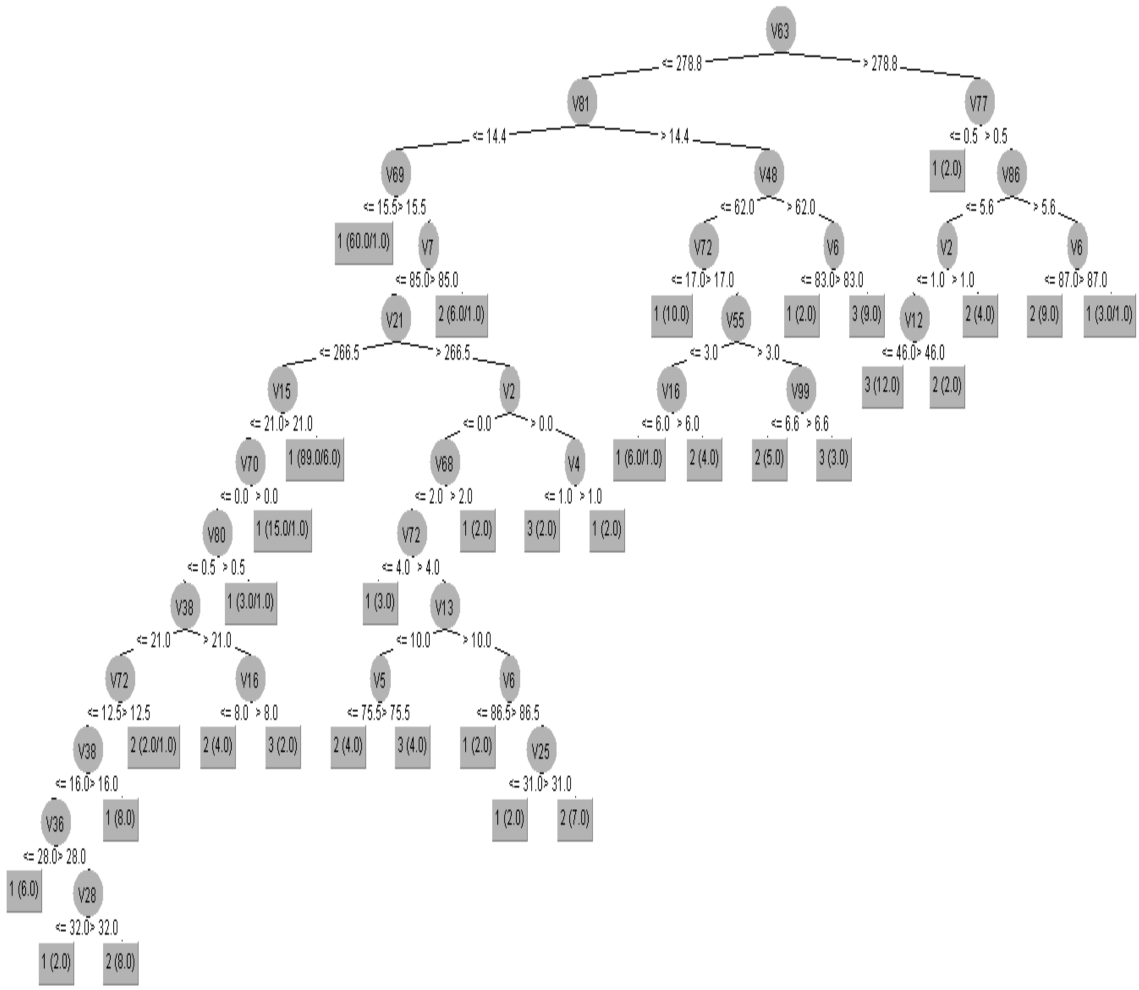

Figure 11: J48 (C 0.25) pruned decision tree of all weather-based indicators of climate generated on WEKA. See appendix IV for the detailed J48 (C 0.25) pruned decision tree and appendix V for the meanings of each variable.

As seen in figure 12, there were 304 instances of which in the 10-fold cross-validation, 201 (66.1%) were correctly classified whereas, in the training set, 291 (95.7%) were correctly classified with a precision of 0.649 and 0.958, respectively. The average of the percentage of the captured data (recall), classified in a category in the training set was 0.957 and 0.661 for the cross-validation test option. The F-measure, the harmonic mean of the precision and recall, was higher in the training set (0.956). In all cases, 10-fold cross-validation and training set, the percentage of time an instance was correctly classified, ROC Area (shows the performance of classifiers, values recorded were higher than 0.5, the threshold for a random classifier). The ROC area for the training set (0.974) was higher than that of the 10-fold cross-validation (0.647). The training set option had the highest value of kappa statistic at 0.908 whereas the cross-validation test recorded a value of 0.2821.

```
Number of Leaves  :     34

Size of the tree :      67


Time taken to build model: 0.04 seconds

=== Stratified cross-validation ===
=== Summary ===

Correctly Classified Instances         201               66.1184 %
Incorrectly Classified Instances       103               33.8816 %
Kappa statistic                          0.2821
Mean absolute error                      0.2395
Root mean squared error                  0.4642
Relative absolute error                 74.2894 %
Root relative squared error            115.833  %
Total Number of Instances              304

=== Detailed Accuracy By Class ===

                 TP Rate  FP Rate  Precision  Recall   F-Measure  MCC      ROC Area  PRC Area  Class
                 0,821    0,454    0,794      0,821    0,808      0,375    0,687     0,770     1
                 0,258    0,140    0,320      0,258    0,286      0,128    0,499     0,245     2
                 0,429    0,093    0,375      0,429    0,400      0,317    0,672     0,259     3
Weighted Avg.    0,661    0,348    0,649      0,661    0,654      0,318    0,647     0,604

=== Confusion Matrix ===

   a   b   c   <-- classified as
 170  24  13 |   a = 1
  34  16  12 |   b = 2
  10  10  15 |   c = 3
```

(a)

```
Number of Leaves  :     34

Size of the tree :      67

Time taken to build model: 0.04 seconds

=== Evaluation on training set ===

Time taken to test model on training data: 0 seconds

=== Summary ===

Correctly Classified Instances         291               95.7237 %
Incorrectly Classified Instances        13                4.2763 %
Kappa statistic                          0.908
Mean absolute error                      0.0485
Root mean squared error                  0.1558
Relative absolute error                 15.0667 %
Root relative squared error             38.888  %
Total Number of Instances              304

=== Detailed Accuracy By Class ===

                 TP Rate  FP Rate  Precision  Recall   F-Measure  MCC      ROC Area  PRC Area  Class
                 0,995    0,113    0,949      0,995    0,972      0,909    0,972     0,978     1
                 0,855    0,008    0,964      0,855    0,906      0,886    0,967     0,927     2
                 0,914    0,000    1,000      0,914    0,955      0,951    0,995     0,976     3
Weighted Avg.    0,957    0,079    0,958      0,957    0,956      0,909    0,974     0,967

=== Confusion Matrix ===

   a   b   c   <-- classified as
 206   1   0 |   a = 1
   9  53   0 |   b = 2
   2   1  32 |   c = 3
```

(b)

Figure 12: Results of the J48 classifier decision tree for; (a) 10-fold cross-validation and (b) training set.

Table 2: Summary of the classification accuracy statistics for the two algorithms runs above.

Test option	**Correctly classified instances %**	**Kappa Statistic**	**Average ROC Area**
Cross-validation	66.1184	0.2821	0.647
Training set	95.7237	0.908	0.974

From this summary, it can be seen that in all classification accuracy results, the training set had better scores as compared to the cross-validation test.

3.2. Simulation study

To evaluate the impact of climate change in the promotion of the epidemics of *Puccinia triticina* responsible for brown rust on winter wheat, the results of the simulation analysis was as follows:

3.2.1. Temporal integration of Rue

The temporal integration of RUE was used as an indicator for summarising the RUE over each of the 150 years. From the simulation, the prediction indicates an irregular pattern in the use of radiation over the one hundred and fifty (150) years. The average temporal integration of RUE was 391 g MJ^{-1}.d over the years. The maximum would be 501.6 g MJ^{-1}.d in 2080 and the minimum temporal integration of RUE was 240.79 g MJ^{-1}.d in 1961 (figure 13).

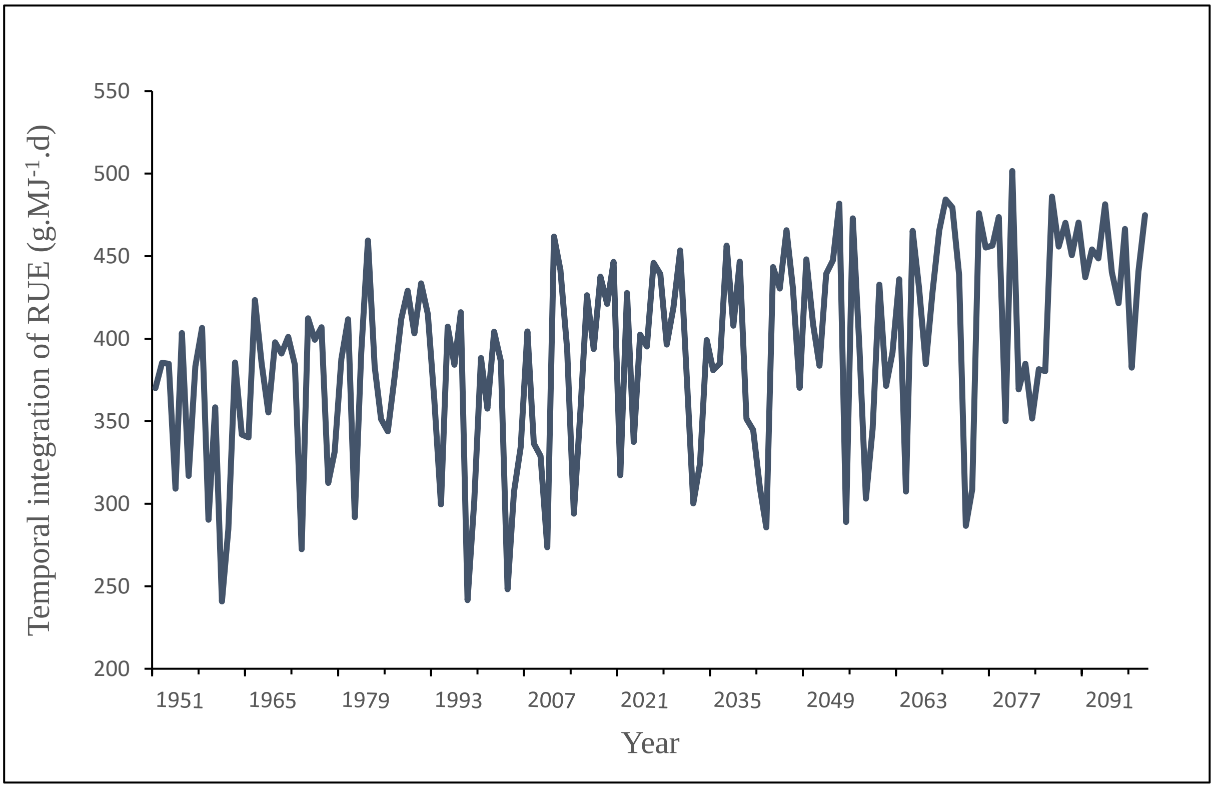

Figure 13: The temporal integration of RUE from January 1st to August 7th for each year of the 1951–2100 period.

3.2.2. Thermal time

Thermal time gives information about the daily increase in temperature over some time. From the simulations, it is predicted that thermal time over the years is inconsistent and it also indicates that in 2042, it will reach a peak at 3008 °C.d. The average thermal time predicted is 2312 °C.d and the minimum for the years recorded is 1777 °C.d in 1970 (figure 14).

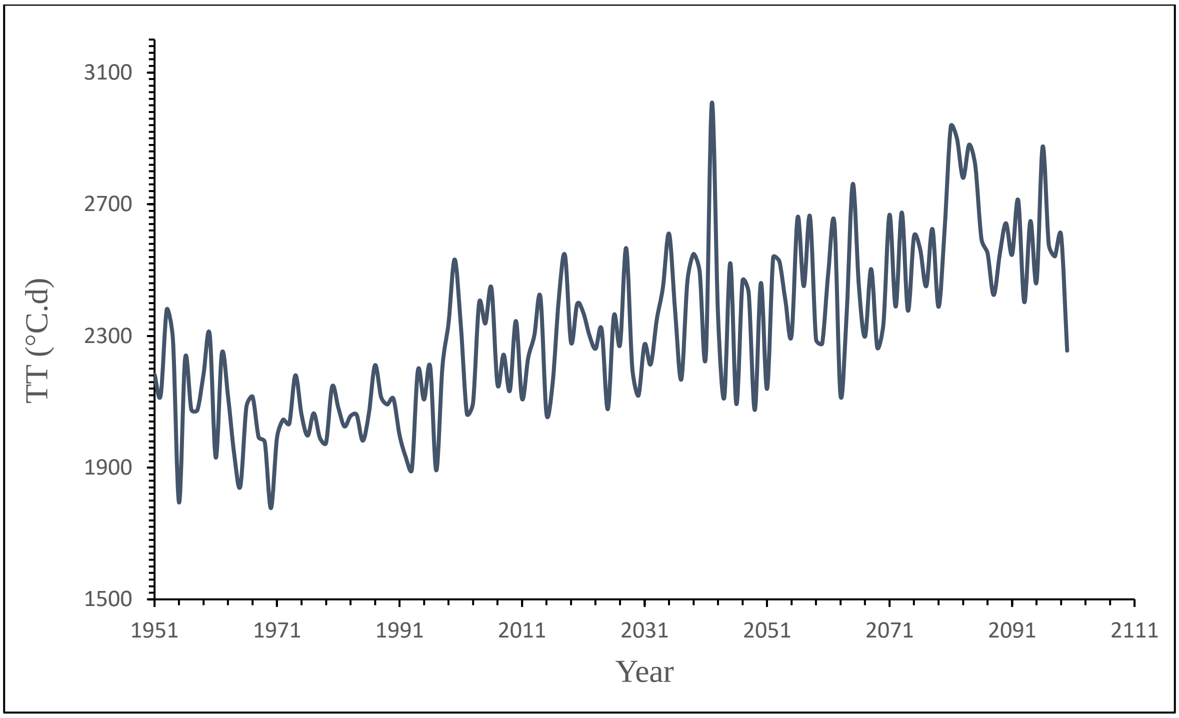

Figure 14: Thermal time with a base temperature of 0°C from January 1st to August 7th for each year of the 1951–2100 period.

3.2.3. Area Under Disease Progress Curve (AUDPC)

AUDPC gives an idea of the predicted disease progression for the 150 years. It can be observed that there is an uneven distribution of disease severity over the one hundred and fifty (150) years. The average AUDPC was 7093 %.d over the years. The maximum was 9859 %.d in 2000 and the minimum AUDPC was 4120 %.d in 1981 (figure 15).

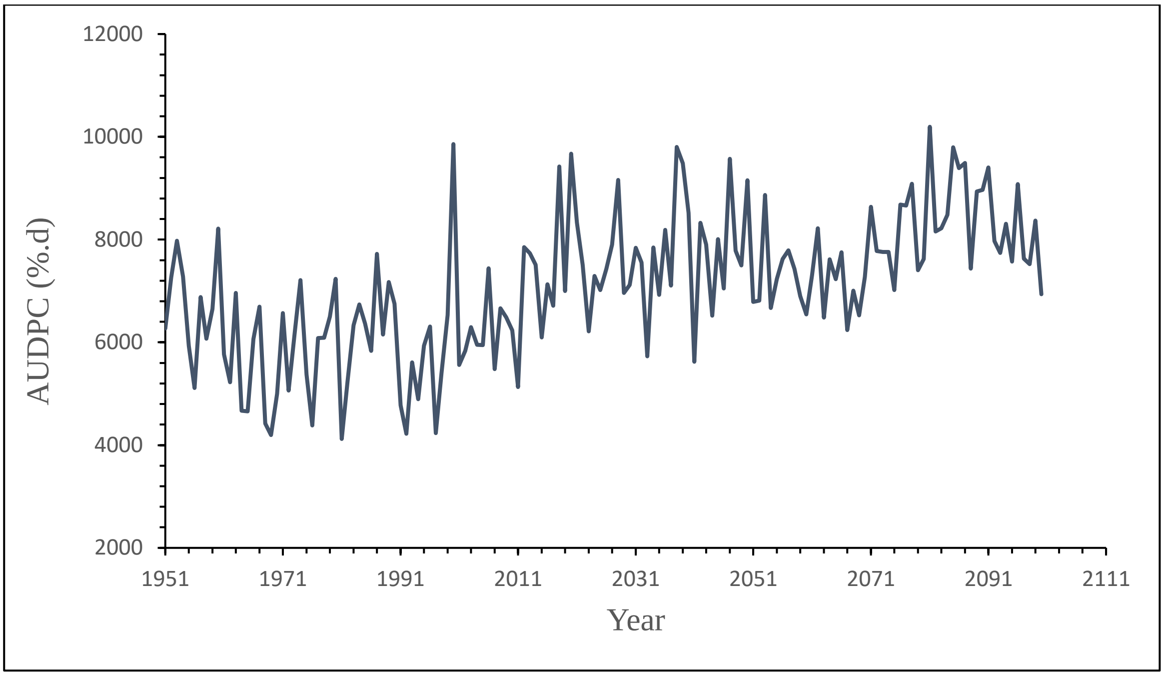

Figure 15: AUDPC of brown rust from January 1st to August 7th for each year of the 1951–2100 period.

3.2.4. The estimated yield for 1951–2100

To assess the risk of the biotic stress on winter wheat and the associated damages, the yield was simulated. The simulated yield was calculated using the data of the aboveground biomass from STICS-MILA and the biomass variables (with the exception of root biomass) simulated by WHEATPEST. For the ear biomass, only 85% of it was used for the calculation. For predictions, it can be noted that simulated yield varied across the years. For the 150 years, the average yield was 1235 g m^{-2}. The highest yield recorded is predicted to be 1666 g m^{-2} in 2065 and the lowest yield was 651 g m^{-2} in 1998 (figure 16).

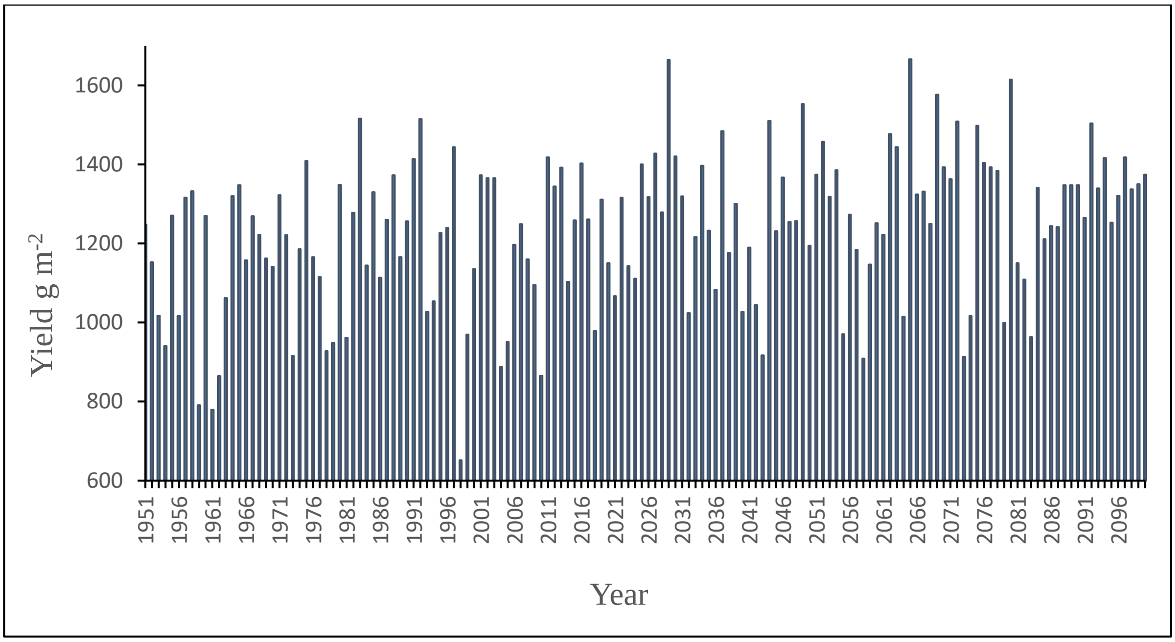

Figure 16: Simulated yield over from January 1st to August 7th for each year of the 1951–2100 period.

3.2.5. Analysis for one scenario (1951)

3.1.5.1 Effects of tmax and tmin on the development of brown rust

In figure 17 below, it can be seen that there is a steady rise in temperature from the beginning of the year to the end of the growing season. BRS remains below 1 for a long time and only begins to develop into a new phase in the latter part of May. BRS reaches a peak (100%) at increased temperatures in the second half of June and remains that way till the wheat is harvested. The highest temperature for tmax was recorded on the 26th of June at 29.2°C with a 100% severity of brown rust while the lowest tmax, -8.4°C was recorded on 1st January with a BRS of 0%. For tmin, the same trend is noticed as the highest temperature was on the 19th of June at 17.2°C with a BRS of 97.3% while the lowest tmin recorded was -12.4°C on the3rd of January with a BRS of 0%. For both cases, BRS increased when temperatures were between 15℃ and 25℃.

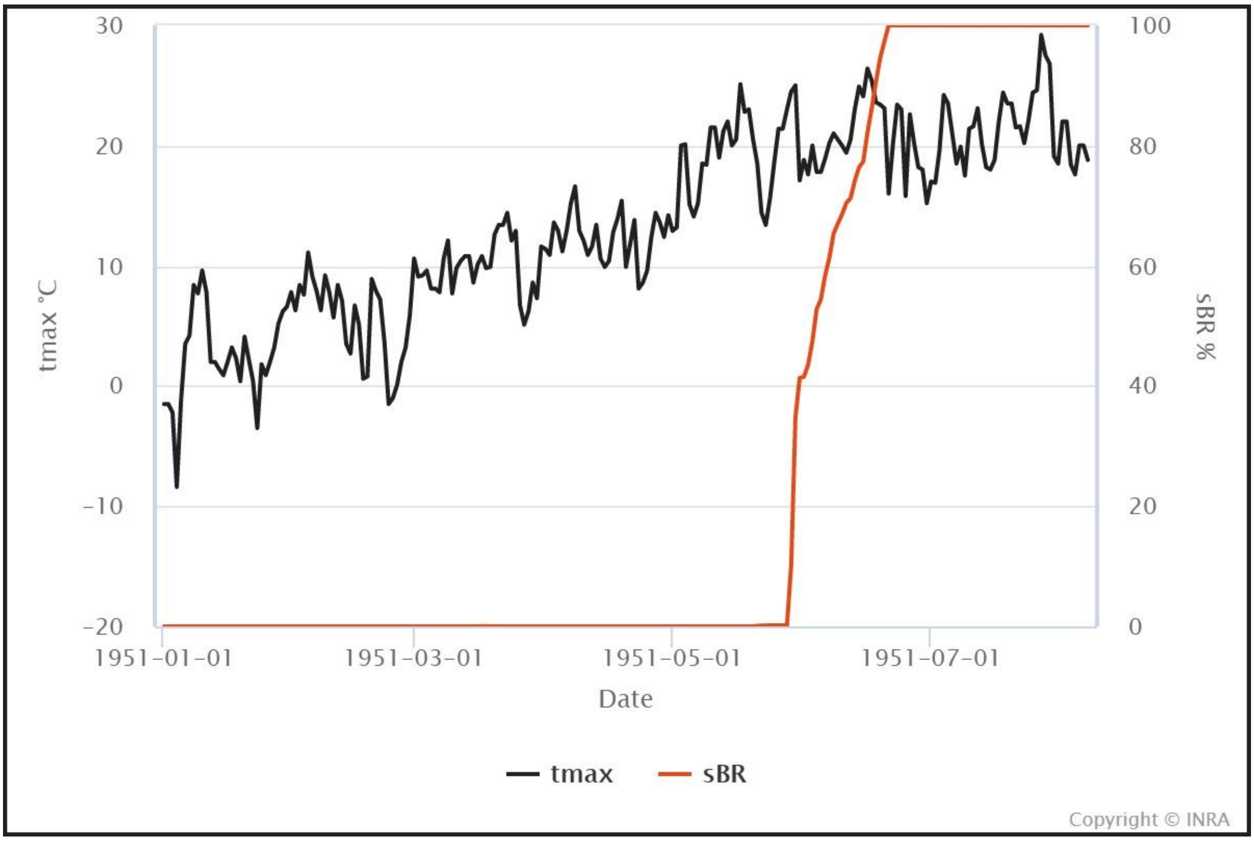
30
20
10
0
-10
-20
tmax °C
100
80
60
40
20
0
sBR %
1951-01-01
1951-03-01
1951-05-01
1951-07-01
Date
tmax
sBR
Copyright © INRA

(a)

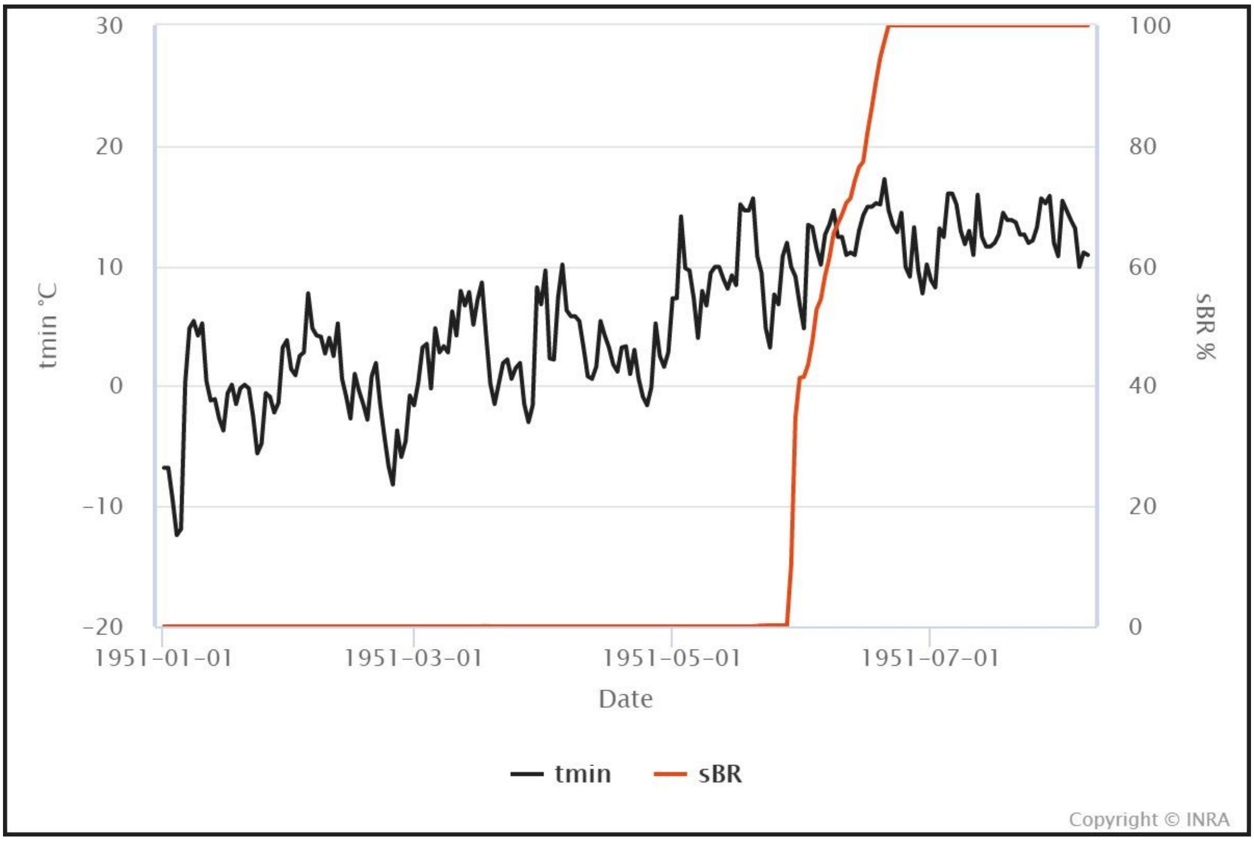
30
20
10
0
-10
-20
tmin °C
100
80
60
40
20
0
sBR %
1951-01-01
1951-03-01
1951-05-01
1951-07-01
Date
tmin
sBR
Copyright © INRA

(b)

Figure 17: Dynamics of brown rust for tmax and tmin variables for one scenario (1951). (a) tmax, (b) tmin.

3.1.5.2 RUE

In figure 18, there are fluctuations in RUE at the beginning of the development phase of the crop (flowering and milk stage). Rue decreases towards the end of April till May and starts to increase and reaches the highest point of 4.033 g MJ^{-1} on the 29th of June. The lowest RUE value recorded was 0 on the day of harvest (7th August).

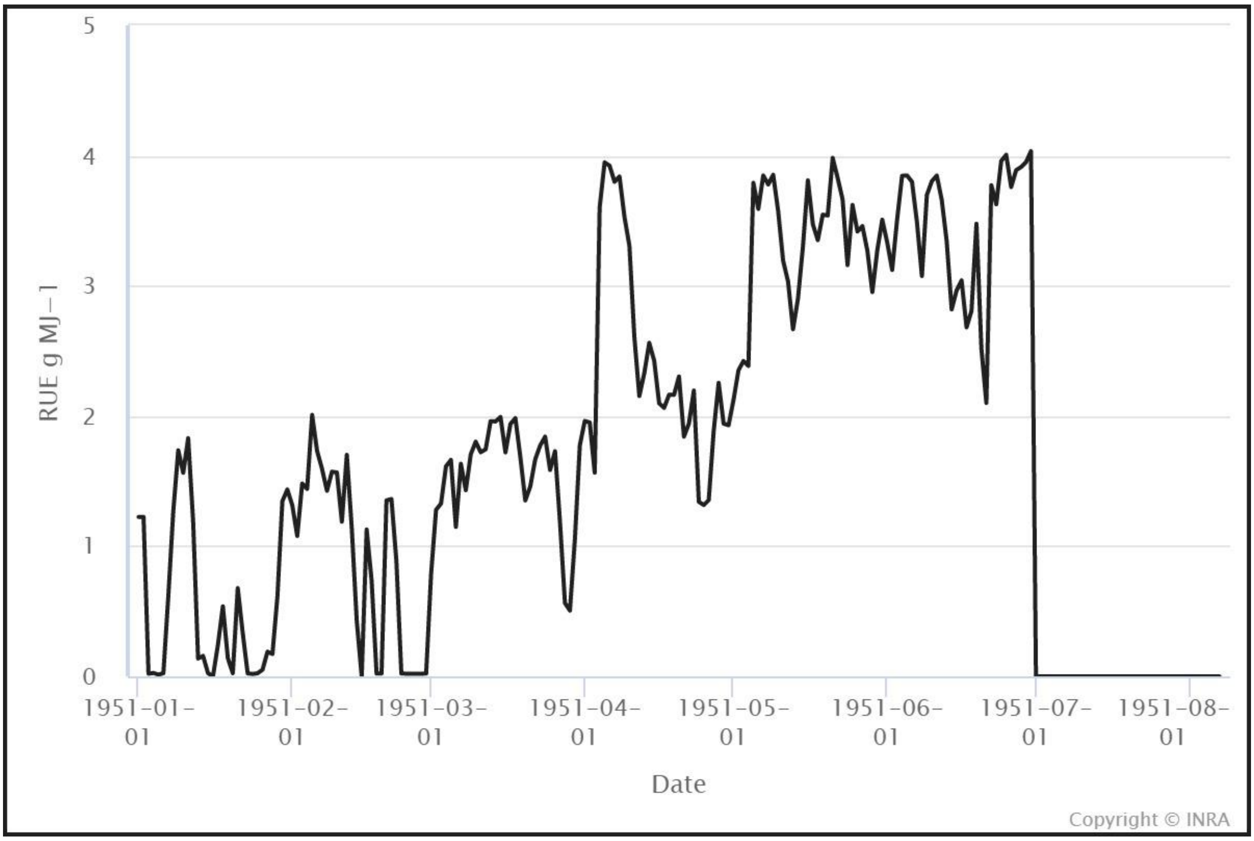

Figure 18: The dynamics of RUE in 1951 from January 1st to August 7th (harvest).
The 0 value recorded was at harvest.

3.1.5.3 State variables (biomass) for the 1951 simulation

Biomass production varied across the year 1951 and this production was proportional to the RUE. The start of the year recorded the low production of biomass for all variables as compared to the later phase of development. Biomass production starts increasing and then remains stable and for some variables, it later decreases at the end of the development phase. For ear biomass, at the beginning of the development phase of the wheat, it recorded a value of 0 and recorded the highest value at 177928 g m^{-2} for all variables at the end of the growth period. Leaf biomass was 10 g m^{-}

^{2} at the start of the year and reached 22 g m^{-2} at the end of the growth period. Stem biomass steadily increases, reaches a peak of 28086 g m^{-2} in May, and records the lowest biomass ($9.35*10^{-5}$ g m^{-2}) for all variables at the end of the development phase. For root biomass, its start value was 5 g m^{-2}, however, it increases along the cycle to 3188 g m^{-2} and then remains stable till the end of the development phase of the wheat (figure 19).

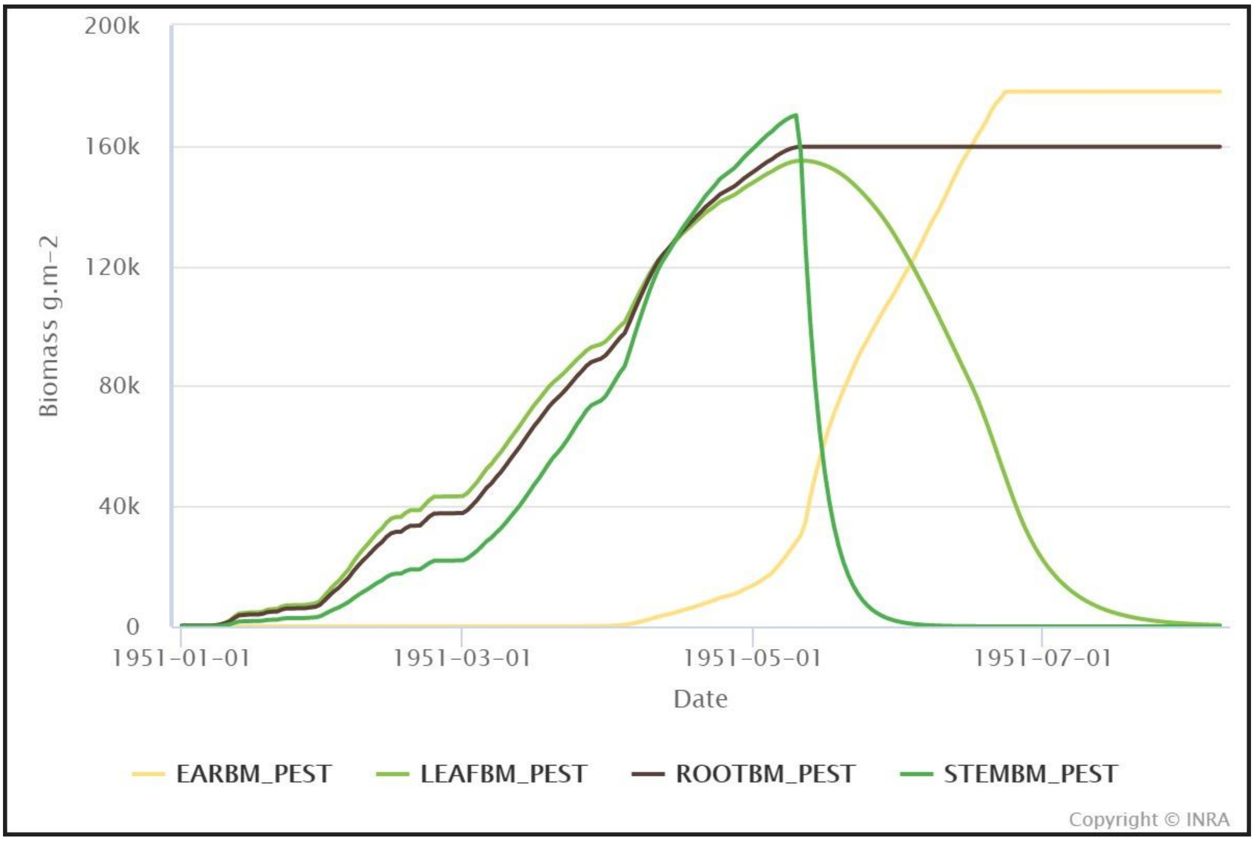

Figure 19: The dynamics of the output variables (leaf, stem, root, and ear biomass) in 1951.

4. CHAPTER 4: DISCUSSION

4.1. Warning bulletins

4.1.1. Evaluation of the model produced by the J48 classifier

In all cases, 10-fold cross-validation and training set, for the ROC area/AUC (Area Under Curve) (shows the performance of classifiers, values recorded were higher than 0.5, the threshold for a random classifier). This means that the classifiers in both tests had good performance rates. However, the ROC Area of the training set classifier (0.974%), close to 1 indicates the better performance of the test option. Narkhede (2018), reports that AUC close to 1 is an excellent model with a good degree of separability and that a random prediction is made when ROC area = 0.5.

Moreover, the reliability of the classifier was tested by the kappa statistic value. McHugh (2012) confirms that in testing reliability either by intrarater or interrater testing, the kappa statistic is very essential for this purpose and this signifies how well the data collected represents the variables measured in the study. Hence, the highest value of kappa statistic at 0.908 for the training set option according to Cohen (1960) suggests a perfect agreement while that of the cross-validation test (0.2821) indicates just a fair agreement.

4.1.2. Predictions and accuracy assessment

From the model produced, the variables that were highly significant to differentiate among classes were; V63 (med,tp,ther5,t1), V81 (med,moy,tn,t3) and V77 (med,j,tx,sup32,t3) followed by V69 (med,j,tx,sup25,t3), V48 (med,sin,tm5<25,t2) and V86 (med,tn,t4). Of all 108 attributes, only twenty-six (26) were captured to be segregated among classes (having an impact on BRS). The other 23 variables to be captured by the model as having an impact on the development of BRS were; V 7, V21, V15, V70, V80, V38, V72, V36, V28, V16, V68, V13, V5, V6, V25, V2, V4, V55, V99, and V12. See appendix V for the meanings of each attribute.

From the test options, it can be deduced that all attributes that were found highly significant to be segregated among classes (having an impact on BRS) were all indicators of temperature V63 (med,tp,ther5,t1– median of the thermal time (5°C) during t1), V81 (med,moy,tn,t3– median of daily average minimum temperatures in t3), V77 (med,j,tx,sup32,t3– median of the number of days with tmax above 32°C in t3), V69 (med,j,tx,sup25,t3– median of the number of days with tmax above 25°C in t3), V48 (med,sin,tm5<25,t2– median of the temporal integration during t2 of the sin2 function (0 when temp is below 5°C or above) and V86 (med,tn,t4– median of minimum temperatures in t4). Maximum, minimum temperatures (V81, V86, and V69) between 5 and 25°C or above 25°C and thermal bases of 5°C (V63and V48) predicted to have an impact on BRS is expected as optimal temperatures for the development and progress of the disease is between this range (Kolmer, 2017). However, the prediction of average temperature above 32 °C in July–September (V77) affecting BRS could be a negative impact. As Barrera et al. (2013), reported that temperatures above 32 °C declined severe epidemics of brown rust in sugarcane.

Aside from the indicators of temperature, some indicators of rainfall and relative humidity were captured in the prediction to have an impact on BRS: however, these impacts were not significant. Examples of such attributes are; V7 (med,j,hr,sup70,t1– median of the number of days when relative humidity is above 70% during the 1st trimester), V21 (med,cum,p,t3– median of the cumulative rainfall during the 3rd trimester), V15 (med,j,hr,sup90,t1– median of the number of days when relative humidity is above 90% during the 1st trimester), V12 (med,j,hr,sup80,t2– median of the number of days when relative humidity is above 80% during the 2nd trimester) and V38 (med,j,p,sup5,t4– median of the number of days with rainfall above 5mm during the 4th trimester). This finding is in line with Junk et al. (2016), who confirm that other factors that aid the progress and infection of the disease are rainfall and humidity.

4.2. Simulation study

4.2.1. Climate change promotes the epidemics of *Puccinia triticina* responsible for brown rust on winter wheat

From the simulation analysis, it can be predicted that temperatures would continue to rise over the 150 years for the location, Mons. The increase in the thermal time for the 150 years is also an indicator of this basis. This corresponds to the report by Asseng et al. (2009) that states that in the past few decades, the average global temperatures have increased and have been forecasted to continue with the incidence of hot days.

The predicted increase in temporal integration of RUE along the years can be attributed to the increased temperatures predicted. This is because RUE is positively proportional to increased temperatures. This has been reported by the study conducted by Andrade et al. (1993) on the effects of temperature on radiation use efficiency in maize and it was observed that there is a positive and significant association between RUE and mean temperature. Likewise, the increase in RUE could be due to the high nitrogen content of the leaves of wheat due to the use of mulch with pea residues. Nitrogen in wheat has been found to be the most vital nutrient to have an impact on RUE (Muurinen & Peltonen-Sainio, 2006). Willocquet et al. (2008) also confirm that cropping practices can affect RUE and when conditions for development are not favourable, RUE decreases.

For the production of the biomass of root, stem, ear, and leaf, the diversity across the year 1951 was proportional to the RUE. The low production of biomass recorded at the start of the year as compared to the later phase of development was because RUE was low at the beginning of the year: RUE has been found to have a positive impact on biomass production (Murchie & Reynolds, 2013). Ear biomass recorded the highest value (177928 g m^{-2}) for all variables at the end of the growth period because of wheat development. Leaf biomass decreased at the end of the growth period due to leaf senescence and this is in line with the study conducted by Willocquet et al. (2008). Stem biomass steadily increases, reached a peak in May, and drastically decreased at the end of the development phase, having the lowest biomass (9.35*10 -5 g m^{-2}) for all variables and according to Willocquet et al. (2008), this can be attributed to carbohydrate re-mobilization to the ears.

The large values recorded for ear, leaf, stem, and root biomasses is as a result of an error encountered in the simulation analysis. In ModelBuilder (the model used for the simulation analysis), to simulate biomass of ear, leaf, root, and stem, daily global radiation is used as an input variable. However, due to the unavailability of the daily global radiation from the datasets simulated by STICS-MILA, cumulative global radiation was used as an alternative. The large values of cumulative global radiation affected the values for the various biomasses; hence, resulting in the huge values recorded for leaf, stem, root, and ear biomass.

Climate change poses great threats to the development of brown rust in winter wheat as seen in the simulation studies. AUDPC also increases over the years and this is in line with the claim from the study conducted by Chakraborty and Newton (2011) that states that climate change affects the incidence and development of crop diseases and changes the geographic dissemination of pathogens. In the study for Mons, the development of brown rust was affected by temperature and as observed, the predicted increase in temperature over the 150 years would result in an increase in BRS. Besides, both cases of tmax and tmin recorded in the scenario of 1951, increased disease severity rates when temperatures were above 15°C. This finding corresponds with the study conducted by Kolmer (2017), who reported that the optimum conditions for the development of brown rust are dewy environments and mild temperatures (15°C–25°C) usually during the flowering phase of hosts.

Furthermore, mulch generates humidity and plays a significant role in soil moisture conservation by changing the microclimate of the soil. These changes contribute to the prevention of the growth of weeds, increasing infiltration, and reducing evaporation during the growing season of crops (Teame et al., 2017). Nevertheless, according to Junk et al., (2016), some factors that contribute to the development of brown rust are; relative humidity, air temperatures, and precipitation, hence, the increase in the severity of the disease when the mulch of pea was used as seen in the simulation study can be attributed to this fact. This result is also in line with the study conducted by Devallavieille-Pope et al. (2002) which states that the brown rust disease is influenced by three main weather factors, namely, humidity, temperature, and wind, and as a result, this affects the frequency and severity of the disease (Shaw et al., 2008). However, for this simulation analysis, wind was not considered due to the unavailability of the dataset.

4.2.2. The risk of brown rust on winter wheat

One of the objectives of this research was to find out the risk of this biotic stress on winter wheat and if the associated damages could be quantified: from the simulation, it can be predicted that wheat yields would be indirectly affected by brown rust. This indirect impact is as a result of the direct effect of increased temperatures that would aid the development of the disease. Similarly, the study conducted by Brisson et al. (2010), showed that, in France, during grain filling, high temperatures result in reduced wheat yields and due to climate change, in the future, heat stress will increase throughout grain filling (Gouache et al., 2012). Moreover, it can be seen from the simulation analysis that yield decreased in certain years where temperatures and BRS were high. This is expected as it has been reported that, *Puccinia triticina* is a vital pathogen in wheat cultivation that causes substantial losses in cultivated areas on a global scale (Kolmer, 2005). Correspondingly, Robin et al. (2018), stated that yield losses can reach up to 70% in severe cases of brown rust development if it is not controlled due to the results of reduced kernel biomass and kernel number per head. The large values recorded for the simulated yield is as a result of the huge values of leaf, stem, root, and ear biomass due to the error of using cumulative global radiation instead of daily global radiation.

Besides reducing the yield of wheat, this indirect impact of BRS could affect the quality of the grains. On a national scale, this could be an issue because this can contribute to nutrition insecurity due to the lack of quality cereal grains as according to Gouache et al. (2012), several studies in France show a negative relationship between rising temperatures and crop yields for wheat, maize, and barley (Lobell et al., 2011). Also, the resilience of cultivars used as germplasms could be affected. Lopes et al. (2018), confirmed that sporadic weather conditions associated with rising temperatures and rainfall cause specific challenges for wheat producers as this can decrease improvements in the genetics of winter wheat.

Although in certain instances, where temperatures were high and yield still increased, such as predicted for 2065, this could be attributed to high carbon dioxide concentration due to high temperatures. Meteorological factors, including increasing temperatures, altering precipitation regimes, and elevated levels of atmospheric carbon dioxide, have been reported to influence crop production biophysically (Parrya et al., 2004). Broberg et al. (2019) confirm the non-linear yield response of increased carbon dioxide levels on wheat.

The associated risk can be quantified given the scenario and weather data used for this simulation. The quantification can be done considering different situations of BRS:
No disease: 0
Low severity: 20
Intermediate severity: 50 and above
High severity: 80 and above
This quantification is only considered for the dataset used for this simulation analysis and might change depending on several factors under certain conditions and cropping practices.

4.3. How to adapt cropping practices to control the development of the disease

NASA reports that the period for crop development is prolonged when temperatures are warm, and this implies that crops will need extra water for development. This change in the weather pattern will then result in short and less extreme winters that are not strong enough to kill dormant pests, hence, resulting in severe infestations that lead to massive yield and quality loss in crops (NASA, 2010). This, therefore, instigates the need to find alternate cropping practices that reduce or inhibit the development of brown rust.

Gouache et al. (2012) propose strategies like using improved cultivars (earlier heading cultivars) and modifying sowing dates. Also, phenology and heat stress focused breeding programs as studied by Olesen et al. (2011), have the potential to reduce the negative impact of climate change on wheat production. Therefore, integrating management practices that ensure resource use efficiency as well as increase the hardiness of wheat would be a step towards making wheat fields less susceptible to the disease. Likewise, incorporating practices that aid evapotranspiration and, reduce humidity and warmth can be very beneficial as these factors promote the development of the disease.

Finally, using unconventional control methods such as biological controls or using integrated approaches to prevent leaves and the wheat plant in general from being susceptible to brown rust would be a good option to eliminate and suppress or reduce the disease development and also the impact of the disease while protecting the environment. Moricca and Ragazzi (2008), report the ecological compatibility of biological control of rust diseases as it conserves the environment and human health without the release of harmful elements into the ecosystem.

4.4. Contribution of findings to different spatial and temporal levels

There are several benefits to be derived from this study and these can contribute to future developments as well as solve some current agricultural challenges (over time and across future generations). Challenges in building resilient and sustainable food and farm systems can be alleviated with some findings of this study.

At the field-level, identifying promoters of this biotic stress and eliminating or reducing these promoters can lead to improved agroecosystems. This study gives insight into the soil-crop-pathogen relationship in the wheat cultivation agroecosystem in Mons. In this study, it is observed that soils with higher nitrogen contents contribute to an increase in RUE, and increased RUE is a good driver of photosynthesis. The study conducted by Murchie and Reynolds (2013) shows the importance of RUE to photosynthesis in the production of biomass and the rate of growth. Also, through predictions, farmers can plan ahead of time as well as put in place good management measures. Farmers can decide on when to sow (either considering climatic conditions or crop characteristics) and use practices that suppress the development of BRS. All these measures can lead to increased productivity at the farm-level and increase the income of wheat growers in Mons which will eventually better their livelihoods.

At the national level, if these predictions are adopted, BRS would be well managed and productivity and the quality of wheat could be improved. This will result in improved resilient varieties and quality wheat grains would help enhance the diets of the population while ensuring nutrition security since wheat is one of the most consumed cereals in France and also used as food for livestock. Shewry and Hey (2015) confirm the economic impact of wheat and its contribution to the nourishment of individuals and livestock. When productivity is enhanced, the excess wheat can be exported to countries that do not produce wheat or even countries that under-produce as it has been reported that in developing countries, the demand for wheat is projected to increase by 60% (CIMMYT, 2017).

Globally, food and nutrition security is an essential policy concern and the present challenge of malnutrition worldwide is a major concern in all countries (Allen & Prosperi 2016). Hence, considering the benefits at the farm and national level and the exportation of excess to countries who are in demand, global food security can be ensured. Moreover, improvements can be made on models to facilitate accurate predictions in farm systems and improve food systems to secure food for now and future generations. Allen and Prosperi (2016) also suggest that government institutions should formulate policies and monitor the advancement of sustainability of farm and food systems. This would ensure developments by detecting and modelling the fundamental properties of these systems; hence, policies should be put in place to facilitate modelling as it is time convenient and more cost-effective for making predictions for long years as compared to actual fieldwork.

5. CHAPTER 5: CONCLUSION

In accordance with other studies, it can be noted that from this research, climate change promotes the epidemics of brown rust. Temperatures above 15 °C greatly promote the development of the disease. Scenarios from this study indicate that till 2100, temperatures would continue to rise, hence, RUE and disease severity of brown rust would also increase. Relative humidity between 70% and 90% were also found to promote the epidemics of brown rust. Also, it can be deduced that RUE increases when nitrogen content is high. The associated risk of the development of the disease is its impact on yield. Yield is predicted to be impacted either negatively or positively by climate change and simulation analysis is a better option to predict scenarios for the future as this analysis is time convenient. AUDPC was convenient in quantifying the brown rust severity in Mons over many years. However, to fully predict and quantify brown rust severity for the 150 years in Mons, results for other cropping practices simulated by STICS-MILA for the location should also be studied to understand the impact of adaptation strategies on the disease dynamics.

Furthermore, many improvements could be made in the simulation analysis by replacing RUE as an input variable with other readily available data such as the use of soil properties as RUE was a limitation because it is not easy to obtain. A sub-model that predicts RUE could be produced to ease this limitation.

Also, a more comprehensive study for a publication on the model created for the warning bulletins would be undertaken by Dr. Jean-Noël Aubertot (INRAE), Dr. Marie-Hélène Robin (Ecole d'Ingénieurs de Purpan), Dr. Gustavo Azzimonti (former post-doc INRAE), Dr. Camilo Corrales (post-doc INRAE) and myself to upgrade the model using larger datasets in order to give a better prediction quality and explanations of the contributions of the various weather indicators to the development of brown rust severity.

REFERENCES

Allen, T., Prosperi, P. (2016). Modelling sustainable food systems. *Environmental Management,* 57: 956–975.

Anderson, R. L., Soper, G. (2003). Review of volunteer wheat (Triticum aestivum) seedling emergence and seed longevity in soil. *Weed Technology,* 17: 620-626.

Andrade, F., Uhart, S., Cirilo, A. G. (1993). Temperature affects radiation use efficiency in maize. *Field Crops Research,* 32 (1–2):17-25.

Anikster, Y., Eilam, T., Bushnell, W. R., Kosman, E. (2005). Spore dimensions of Puccinia species of cereal hosts as determined by image analysis. *Mycologia*, 97: 474–484.

Araya, A., Hoogenboom, G., Luedeling, E., Hadgu, K., Kisekka, I., Martorano, L. (2015). Assessment of maize growth and yield using crop models under present and future climate in south-western Ethiopia. *Agricultural and Forest Meteorology*, 214-215: 252-265.

Asseng, S., Foster, I., Turner, N. C. (2009). Has the impact of temperature variability on wheat production been underestimated? National Seminar on Climate Change Adaptation Strategies in Agriculture, sponsored by ISRO, Govt. of India and Kerala Agricultural University 3-4 December 2009, Kerala Agricultural University, India.

Asseng, S., Foster, I., Turner, N. C. (2011). The impact of temperature variability on wheat yields. *Global Change Biology*, 17: 997–1012.

Aubertot, J.N., Robin, M.H. (2013). Injury Profile SIMulator, a qualitative aggregative modelling framework to predict crop injury profile as a function of cropping practices, and the abiotic and biotic environment. I. Conceptual bases. *PLOS One,* 8:e73202. doi:10.1371/journal.pone.0073202.

Azzimonti G. (2012). Diversification de la résistance quantitative la rouille brune du blé, à partir de la caractérisation des composantes de la résistance. *PhD thesis*, AgroParisTECH, Paris, France.

Barrera, W., Hoy, J., Li, B. (2013). Effects of temperature and moisture variables on brown rust epidemics in sugarcane. *Journal of Phytopathology*, 161(2): 98-106.

Batts, G. R., Ellis, R. H., Morison, J. I. L., Nkemka, P. N., Gregory, P. J., Hadley P. (1998). Yield and partitioning in crops of contrasting cultivars of winter wheat in response to CO_2 and temperature in field studies using temperature gradient tunnels. *Journal of Agriculture Science,* 130: 17-27.

Béné, C, Oosterveer, P, Lamotte, L. (2019). When food systems meet sustainability– Current narratives and implications for actions. *World Development,* 113, 116–130.

Beniston, M., Stephenson, D. B., Christensen, O. B., Ferro, C. A., Frei, C., Goyette, S., Palutikof,

J. (2007). Future extreme events in European climate: an exploration of regional climate model projections. *Climatic change*, 81 (1): 71-95.

Bohanec, M., Messean A., Scatasta S., Angevin F., Griffiths B. (2008). A qualitative multi-attribute model for economic and ecological assessment of genetically modified crops. *Ecological Modelling*, 215: 247–261.

Bohanec, M. (2017). DEXi: A program for multi-attribute decision making version 5.02. Available at: https://kt.ijs.si/MarkoBohanec/dexi.html (accessed: 03.24.20)

Bolton, M. D., Kolmer, J. A., Garvin, D. F. (2008). Wheat leaf rust caused by Puccinia triticina. *Molecular plant pathology*, 9 (5): 563–575. https://doi.org/10.1111/j.1364-3703.2008.00487.x (accessed: 03.24.20)

Briggle, L.W. (1980). Origin and botany of wheat. In Häfliger, E. (ed.), *Wheat documenta cibageigy*, pp 6-13. Basle, Switzerland.

Brisson, N., F. Levrault. (2010). Livre vert du projet CLIMATOR - changement climatique, agriculture et forêts en France : simulations d'impacts sur les principales espèces. ADEME éditions.

Brisson, N., Gate, P., Gouache, D., Charmet, G., Oury, F.-X., Huard, F. (2010). Why are wheat yields stagnating in Europe? A comprehensive data analysis for France. *Field Crops Research*, 119: 201–212.

Broberg, M., Högy, P., Pleijel, H. (2019). Effects of elevated CO_2 on wheat yield: non-linear response and relation to site productivity. *Agronomy*, 9 : 243.

Caubel, J., Launay, M., Ripoche, D., Gouache, D., Buis, S., Huard, F., Huber, L., Brun, F., Bancal, M. O. (2017). Climate change effects on leaf rust of wheat: Implementing a coupled crop disease model in a French regional application. *European Journal of Agronomy,* 90: 53–66.

Chakraborty, S., Newton, A. C. (2011). Climate change, plant diseases and food security: an overview. *Plant Pathology*, 60: 2–14.

Church, J. A., Clark, P. U., Cazenave, A., Gregory, J. M., Jevrejeva, S., Levermann, A., Merrifield, M. A., Milne, G. A., Nerem, R. S., Nunn, P. D., Payne, A. J., Pfeffer, W. T., Stammer D., Unnikrishnan, A. S., 2013. Sea Level Change. In Stocker, T. F., Qin, D., Plattner, G. K., Tignor, M., Allen, S. K., Boschung, J., Nauels, A., Xia, Y., Bex V., Midgley P. M. (ed.) *Climate change 2013: The Physical Science Basis. Contribution of Working Group I to the Fifth Assessment Report of the Intergovernmental Panel on Climate Change*. Cambridge University Press, Cambridge, United Kingdom and New York, NY, USA.

Curtis, B. C. (1992). Wheat in the world. Available at: http://www.fao.org/3/y4011e04.html

(accessed: 03.15.20)

Cohen, J. A (1960). Coefficient of agreement for nominal scales. *Educational and Psychological Measurement,* 20: 37–46.

De Vallavieille-Pope, C., Giosue, S., Munk, L., Newton, A. C., Niks, R. E., Østergård, H., Pons-Kühnemann, J., Rossi, V., Sache, I. (2000). Assessment of epidemiological parameters and their use in epidemiological and forecasting models of cereal airborne diseases. *Agronomie,* 20: 715-727.

Devallavieille-Pope, C., Huber, L., Leconte M., Bethenod, O. (2002). Pre inoculation effects of light quantity on infection efficiency of Puccinia striiformis and P. triticina on wheat seedlings. *Phytopathology*, 92: 1308- 1314.

Eibe, F., Hall, M, A., Witten, I, A. (2016). *The WEKA workbench online appendix for "data mining: practical machine learning tools and techniques",* fourth edition. Morgan Kaufmann Publishers.

El Jarroudi, M., Kouadio, L., Tychon, B., Junk, J., Bock, C., Delfosse, P. (2018). Modelling the main fungal diseases of winter wheat: constraints and possible solutions. In Kimatu, J. N. (ed.) *Advances in Plant Pathology*, pp 1-29. IntechOpen.

Francis, C., Lieblein, G., Gliessman, S., Breland, T. A., Creamer, N., Harwood, R., Salomonsson, L., Helenius, J., Rickerl, D., Salvador, R., Wiedenhoeft, M., Simmons, M., Allen, P., Altieri, M., Flora, C., Poincelot, R. (2003). Agroecology: The ecology of food systems. *Journal of Sustainable Agriculture,* 22 (3): 99-118. doi: 10.1300/J064v22n03_10.

FAO, Benedetti, A. (2019). Transforming food and agricultural systems: a challenge we must face together. Available at: http://www.fao.org/fao-stories/article/en/c/1254608/ (accessed: 03.15.20).

Gate, P., Blondlot, A., Gouache, D., Deudon, O., Vignier, L. (2008). Impacts du changement climatique sur la croissance et le développement du blé en France Quelles solutions et quelles actions à développer? *Oléagineux, Corps Gras, Lipides*, 15: 332–336.

Gouache, D., Le Bris, X., Bogard, M., Deudon, O., Pagé, C., Gate, P. (2012). Evaluating agronomic adaptation options to increasing heat stress under climate change during wheat grain filling in France. *European Journal of Agronomy*, 36 (1): 62–70.

Goyeau, H. & Lannou, C. (2011). Specific resistance to leaf rust expressed at the seedling stage in cultivars grown in France from 1983 to 2007. *Euphytica,* 178: 45-62.

Hirst, J. M. & Hurst, G. W. (1967). Long-distance spore transport. In Gregory, P. H. & Monteith, I. L. (ed.) *Airborne Microbes,* pp. 307-344. Cambridge University Press.

Hubeau, M., Marchand, F., Coteur, I., Mondelaers, K., Debruyne, L., Van Huylenbroeck, G. (2017). A new agri-food systems sustainability approach to identify shared transformation pathways towards sustainability. *Ecological Economics*, 131: 52-63.

IPCC (2009). IPCC Working Group I: The physical science basis of climate change: latest findings to be assessed by WGI in AR5. IPCC. Available at: https://www.ipcc-wg1.unibe.ch/presentations/stocker09unfcccCopenhagendelegatenew.pdf (accessed: 03.21.20).

International Maize and Wheat Improvement Center (CIMMYT) (2017). Wheat. Available at: https://wheat.org/ (accessed: 03.21.20).

Jeger, M. J. & Rollinson, S. L. H. V. (2001). The use of the area under the disease-progress curve (AUDPC) to assess quantitative disease resistance in crop cultivars. *Theoretical and Applied Genetics*, 102: 32-36.

Junk, J., Kouadio, L., Delfosse, P., EL Jarroudi, M. (2016). Effects of regional climate change on brown rust disease in winter wheat. *Climatic Change*, 135: 439–451.

Kolmer, J. A. (2005). Tracking wheat rust on a continental scale. *Current Opinion in Plant Biology*, 8: 441–449.

Kolmer, J. (2013). Leaf rust of wheat: pathogen biology, variation, and host resistance. *Forests*, 4, pp. 70-84. doi: 10.3390/f4010070. USDA-ARS, Cereal Disease Laboratory, St. Paul, MN 55113, USA.

Kolmer, J. A. (2017). Wheat leaf rust: USDA-ARS. Available at: https://www.ars.usda.gov/midwest- area/stpaul/cereal-disease-lab/docs/cereal-rusts/wheat-leaf-rust/ (accessed: 03.21.200).

Leonard, K. J. & Szabo, L. S. (2005). Stem rust of small grains and grasses caused by Puccinia graminis. *Molecular Plant Pathology*, 6: 99–111.

Lobell, D. B., Field, C. B., Cahill, K. N., Bonfils, C. (2006). Impacts of future climate change on California perennial crop yields: model projections with climate and crop uncertainties. *Agriculture and Forest Meteorology*, 141 (2–4): 208-218.

Lopes, M. S., Royo, C., Alvaro, F., Sanchez-Garcia, M., Ozer, E., Ozdemir, F., Karaman, M., Roustaii, M., Jalal-Kamali, M. R., Pequeno, D. (2018). Optimizing winter wheat resilience to climate change in rain fed crop systems of Turkey and Iran. *Frontiers in Plant Science*, 9: 563. doi: 10.3389/fpls.2018.00563.

Luck, J., Spackman, M., Freeman, A., Trebicki, P., Griffiths, W., Finlay, K., Chakraborty, S. (2011). Climate change and diseases of food crops. *Plant Pathology*, 60: 113–121.

Lüthi, D., Le Floch, M., Bereiter, B. Blunier, T., Barnola, JM., Siegenthaler, U., Raynaud, D., Jouzel, J., Fischer, H., Kawamura, K., Stocker, T., F. (2008). High-resolution carbon dioxide concentration record 650,000–800,000 years before present. *Nature*, 453: 379–382.

Mariscal, M., Orgaz, F., Villalobos, F. (2000). Radiation-use efficiency and dry matter partitioning of a young olive (Olea europaea) orchard. *Tree physiology,* 20: 65-72.

McHugh, M. L. (2012). Interrater reliability: the kappa statistic. *Biochemia medica* 22 (3): 276–282.

Ministère de l'Agriculture et de l'Alimentation (2015). Overview of French Agricultural Diversity. https://agriculture.gouv.fr/overview-french-agricultural-diversity (accessed: 03.21.20).

Mishra, A. N., Varma, P. K., Diwali, I. N. (1994). Rust incidence in late-sown wheat (Triticum aestivum). *Indian Journal of Agricultural Science*, 64: 266-267.

Moricca, S. & Ragazzi, A. (2008). Biological and integrated means to control rust diseases. In Ciancio, A. & Mukerji, K. G. (ed.) *Integrated management of diseases caused by fungi, phytoplasma and bacteria*, pp.303-329. Springer Science+Business Media B.V.

Murchie E. & Reynolds M. (2013). Crop radiation capture and use efficiency. In Christou P., Savin R., Costa-Pierce B.A., Misztal I., Whitelaw C. B. A. (ed.) *Sustainable Food Production*. Springer, New York, NY. Availabe at: https://doi.org/10.1007/978-1-4614-5797-8_171 (accessed: 05.24.20).

Muurinen, S. & Peltonen-Sainio, P. (2006). Radiation-use efficiency of modern and old cereal cultivars and its response to nitrogen in northern growing conditions. *Field Crops Research*, 96: 363-373. doi: 10.1016/j.fcr.2005.08.009.

Narkhede, S. (2018). Understanding AUC - ROC Curve. Available at: https://towardsdatascience.com/understanding-auc-roc-curve-68b2303cc9c5 (accessed: 05.24.20).

NASA Earth Observatory (2010). Global Warming. Available at: https://earthobservatory.nasa.gov/features/GlobalWarming/page6.php (accessed: 05.24.20).

NASA. Climate Change: How Do We Know? Available at: https://climate.nasa.gov/evidence/ (accessed: 03.22.20).

Nikolaev, S. V., Zubairova, U. S., Skolotneva, E. S., Afonnikov, D. A., Orlova, E. A. (2019). A system approach to the modelling of fungal infections of the wheat leaf. *Vavilov Journal of Genetics and Breeding*, 1: 100-109. doi: 10.18699/VJ19.468.

NOAA National Centers for Environmental Information, State of the Climate: Regional Analysis for January 2020. Available at: https://www.ncdc.noaa.gov/sotc/global-regions/202001 (accessed: 03.22.20).

Oishmaya, S. N. (2019). "Top Wheat Producing Countries". WorldAtlas. Available at: https://www.worldatlas.com/articles/top-wheat-producing-countries.html (accessed: 03.22.20).

Olesen, J. E., Trnka, M., Kersebaum, K. C., Skjelvåg, A. O., Seguin, B., Peltonen-Sainio, P., Rossi, F., Kozyra, J., Micale, F. (2011). Impacts and adaptation of European crop production systems to climate change. *European Journal of Agronomy*, 34: 96–112.

Papaix, J., Goyeau, H., Cheyron, P. D., Monod, H., and Lannou, C. (2011). Influence of cultivated landscape composition on variety resistance: An assessment based on wheat leaf rust epidemics. *New Phytologist*, 191: 1095-110.

Parrya, M. L., Rosenzweigb, C., Iglesiasc, A., Livermored, M., Fischere, G. (2004). Effects of climate change on global food production under SRES emissions and socio-economic scenarios. *Global Environmental Change*, 14: 53–67.

Pazek K., Rozman C., Bavec F., Borec A., Bavec M. (2010). A multi-criteria decision analysis framework tool for the selection of farm business models on organic mountain farms. *Journal of Sustainable Agriculture*, 34: 778–799.

Pazek K., Rozman C. (2007). The decision support system for supplementary activities on organic farms. *Agricultura (Slovenia),* 5 : 15–20.

Poumadere, M., Mays, C., Le Mer, S., Blong, R. (2005). The 2003 heat wave in France: dangerous climate change here and now. *Risk Analysis*, 25: 6. doi: 10.1111/j.1539-6924.2005.00694.x

Reboud, X., Carpentier, A., Aubertot, J.N., Lemarié, S., Peyrard, N., Turenne, N., Roussey, C., Couture, S., Cellier, V., Gaba, S., Sabbadin, R., Cros, M. J., Toquebeuf, P., Bonroy, O., Barbier, J. M., Charbonnier, E. (2017). Ce que l'épidémiosurveillance apporte ou n'apporte pas encore à la moindre dépendance aux produits phytopharmaceutiques. *Innovations Agronomiques*, 59: 81-91.

Reilly, J., Tubiello, F.N., McCarl, B., Melillo, J. (2001). Impacts of climate change and variability on agriculture. In US National Assessment Foundation Document. National Assessment Synthesis Team, US Global Change Research Program, Washington, DC.

Robert, C., Bancal, M. O., and Lannou, C. (2002). Wheat leaf rust uredospore production and carbon and nitrogen export in relation to lesion size and density. *Phytopathology*, 92: 762-768.

Robert, C., Bancal, M. O., and Lannou, C. (2004). Wheat leaf rust uredospore production on adult plants: Influence of leaf nitrogen content and Septoria tritici blotch. *Phytopathology*, 94: 712-721.

Robin, M.H., Aubertot, J.N., Sache, I. (2015). *IPSIM-WHEAT -WHEAT brown rust, (Injury Profile SIMulator), a hierarchical, aggregative, and qualitative model to predict brown rust severity as a function of cropping practices, soil, climate, and field environment.* 14th International Cereal Rusts and Powdery Mildews Conference, Helsingor, Denmark, 5-8 July 2015, ⟨hal-01405414⟩.

Robin, M.H., Bancal, M.O., Cellier, V., Délos, M., Felix, I., Launay, M., Magnard, A., Olivier, A., Robert, C., Rolland, B., Sache, I., Aubertot J.N. (2018). IPSIM-WHEAT -Web, an online resource for promoting qualitative aggregative hierarchical network models to predict plant disease risk: application to brown rust on wheat. *Plant Disease*, 102 (3): 488 - 499.

Roelfs, A. P., Singh, R. P., Saari, E. E. (1992). *Rust Diseases of Wheat: Concepts and Methods of Disease Management*, pp. 1–81. Mexico, DF: CIMMYT.

Ross Quinlan, J. (1993). C4.5: *Programs for Machine Learning*. Morgan Kaufmann Publishers, San Mateo, CA.

Rossi V., Racca P., Giosuè S., Pancaldi D., Alberti I. (1997). A simulation model for the development of brown rust epidemics in winter wheat. *European Journal of Plant Pathology*, 103: 453–465.

Singh R. P., Huerta-Espino J., Roelfs A. P. (2002). The wheat rusts. In Curtis B. C., Rajaram S, Gómez Macpherson, H. (eds) *Bread wheat: improvement and production, plant production and protection*, series no. 30, pp. 227–249. FAO, Rome.

Shaw, M. W., S. J. Bearchell, B. D. L. &Fraaije. B, A. (2008). Long-term relationships between environment and abundance in wheat of Phaeosphaeria nodorum and Mycosphaerella graminicola. *New Phytologist*, 177: 229-238.

Sheehy, J. E., Mitchell, P. L. & Ferrer, A. B. (2006). Decline in rice grain yield with temperature: models and correlations can give different estimates. *Field Crops Research*, 98: 151–156.

Shewry, P. R., Hey, S. J. (2015). The contribution of wheat to human diet and health. *Food and energy security*, 4 (3): 178–202.

Teame, G., Tsegay, A. & Abrha, B. (2017). Effect of Organic Mulching on Soil Moisture, Yield, and Yield Contributing Components of Sesame (*Sesamum indicum L.*). *International Journal of Agronomy*, 2017: 4767509. doi: 10.1155/2017/4767509.

Tripathi, A., Pohanková, E., Fischer, M., Orság, M., Trnka, M., Klem, K., Marek, M. (2018). The evaluation of radiation use efficiency and leaf area index development for the estimation of biomass accumulation in short rotation poplar and annual field crops. *Forests*, 9 (4): 168.

Tschirley, D., Haggblade, S. & Reardon, T. (2013). *Africa's emerging food system transformation*. Michigan State University, USAID.

United Nations Climate Change (UNFCCC) (2016). The Paris Agreement. Available at: https://unfccc.int/process-and-meetings/the-paris-agreement/the-paris-agreement. (accessed: 03.27.2020).

United Nations Commission on Sustainable Development Goals. Goal 13: Take urgent action to combat climate change and its impacts. Available at: https://www.un.org/sustainabledevelopment/climate-change/ (accessed: 03.27.2020).

United Nations, Shaping our future together. Climate Change. Available at: https://www.un.org/en/sections/issues-depth/climate-change/ (accessed: 03.27.2020).

Wheeler, T., von Braun, J., 2013. Climate change impacts on global food security. *Science*, 341 (6145): 508-513. doi: 10.1126/science.1239402.

Willocquet, L., Aubertot, J.N., Lebard, S., Robert, C., Lannou, C., Savary, S. (2008). Simulating multiple pest damage in varying winter wheat production situations. *Field Crops Research*, 107: 12–28.

Xiao, D., Bai, H. & Liu, D. L. (2018). Impact of Future Climate Change on Wheat Production: A Simulated Case for China's Wheat System. *Sustainability*, 10: 1277.

Zhang, L., Meakin H. & Dickinson, M. (2003). Isolation of genes expressed during compatible interactions between leaf rust (*Puccinia triticina*) and wheat using cDNA-AFLP. *Molecular Plant Pathology*, 4: 469–477.

APPENDICES

Appendix I: 1. Comprehensive literature review

In this section, the keywords of this research, namely "climate change", "wheat" and "brown rust" will be described regarding the current situation and future developments. These keywords will be elaborated and certain components that attribute to these keywords will also be explained. For climate change, after a global view, an emphasis on France will be made and the impacts of climate change on crops in relation to pests will also be described. Wheat, precisely winter wheat, and its production in France, as well as the effects of climate change on production, will be elaborated. A review of brown rust, its life cycle, epidemiology, and symptoms will be made. Then finally, the development of brown rust in wheat production, control strategies, and epidemiological models for brown rust will be reviewed and described.

1.1 Climate change

Every continent is being affected by the consequences of climate change and this has subsequently affected the economies of nations. According to Reilly et al. (2001), climate change is likely to impact developed and developing countries differently, with greater vulnerability emerging in low latitude regions. In the past few decades, the average global temperatures have increased and have been forecasted to continue with the incidence of hot days as reported by Asseng et al. (2009). In history, greenhouse gas emission has reached the highest ever recorded and this has resulted in a massive change in climatic patterns (UN SDGs). These changes in weather patterns pose great threats to agriculture production (Asseng et al., 2011) and threaten the permanency of food security. Climate change caused by greenhouse gas emissions is projected to directly impact agricultural production systems and change the trade pattern and balance of food and food products (Wheeler & von Braun, 2013). The evidence of the increased level of atmospheric carbon dioxide since the Industrial Revolution as reported by Luthi et al. (2008) can be seen in appendix 1. NASA (2010), predicts that towards the end of the 21st century, the average temperature of the earth´s surface could increase between 2°C and 6°C. Apart from this prediction, there are other interesting scenarios presented by NASA that confirm the fast rate of climate change. Some of this evidence is:

i. The worldwide rise in temperature- towards the end of the 19th century, the average temperature of the earth's surface has increased to about 0.9℃. This increase has been attributed to the emissions of gases and increased carbon dioxide levels as a result of human activities.
ii. Rise in sea level- globally, in the last century, the sea level has risen to about 0.2 meters and this is increasing every year. Also, the Intergovernmental Panel on Climate Change

(IPCC) forecasted that by 2099, due to the melting of glaciers and the expansion of seawater as a result of warming, sea levels will rise between 0.18 and 0.59 meters.

iii. Extreme events- records of high temperatures, lower rainfall rates as well as reduced rates of precipitation, wildfires, and droughts. An example is an increased rate of high temperatures in the US.

iv. Ocean acidification and warming- the industrial revolution has led to a 30% acidity increment in the ocean surface waters. Also, the high temperatures recorded globally has resulted in the absorption of heat by oceans.

The UN predicts that soon, solving the problem of climate change will be much harder if it is not tackled today. Risks from the energy, food, and water sectors may overlap spatiotemporally as a result of global warming from 1.5 °C to 2 °C and this would cause new and worsening risks, vulnerabilities, and threats which would affect people all over the world but particularly economically disadvantaged populations (IPCC, 2013). All these implications of climate change have forced the world to seek solutions to this widespread issue. Currently, there are several initiatives to tackle this issue and one major initiative is the Paris Agreement which seeks to ´´to strengthen the global response to the threat of climate change by keeping a global temperature rise in this century well below 2 ℃ above pre-industrial levels and to pursue efforts to limit the temperature increase even further to 1.5 ℃´´. This agreement also fortifies countries to combat the impacts of climate change (UNFCCC, 2016).

1.1.1 A focus on France

Beniston et al. (2007), reports the direct relationship between climate change and flooding in Southern France and its ability to increase the occurrence of storms and heatwaves. Ever Since the beginning of the 20th century, the average temperature in France has risen by 1°C as compared to that of the whole word (0.6℃) (Poumadere et al., 2005). Brisson and Levrault (2010) also reported that, in France, towards the end of the 21st century, warming could rise to around 3.2ºC with a reduction in the rate of rainfall and a contrasting weather pattern (decline in the rate of rainfall during summer).

1.1.2 Effects of climate change on crops in relation to pests

Biophysical and socioeconomic factors are the primary drivers of the agricultural reactions to climate change. Meteorological factors, including increasing temperatures, altering precipitation regimes, and elevated levels of atmospheric carbon dioxide, influence crop production biophysically. (Parrya et al., 2004). Current researches have focused mainly on the direct impacts of climate change, for example on crop growth and the spread of agricultural pests. In 2011, Chakraborty and Newton stated in their study that, climate change affects the incidence and development of crop diseases and changes the geographic dissemination of pathogens. Luck et al. (2011) report the effects of high temperature and increased carbon dioxide concentrations on the development of plant biomass which serve as hosts for fungi growth. The fungi then multiply and cause epidemics and biotic stress at the early stages of plant development when plants are more vulnerable.

NASA also reports that the period for crop development is prolonged when temperatures are warm, and this implies that crops will need extra water for development. This change in the weather pattern will then result in short and less extreme winters that are not strong enough to kill dormant pests, hence, resulting in severe infestations that lead to massive yield and quality loss in crops (NASA, 2010).

1.2 Wheat and its production in France

Wheat (*Triticum spp.*) is a staple food for most people, it is one of the first domesticated crops and is the most cultivated crop with a production rate of over 600 million tons. Wheat is extremely nutritious, containing most nutrients, and is a major source of carbohydrate (Curtis, 1992). This crop grows in most conditions although the optimum conditions for growth are latitudes of 30° and 60°N and 27° and 40°S, 25°C, with the lowest and highest temperatures of 3° to 4°C and 30° to 32°C, respectively with a growing period of 10 to 11 months (Nuttonson, 1955; Briggle 1980). To initiate development, most wheat varieties need a cool climate in their early stages. Globally, the highest producer of wheat is China followed by India, Russia, USA then France (Oishmaya, 2019). In Europe, several diseases such as rusts and blotches cause yield and quality losses yearly with the most common control method being the application of fungicides (Curtis, 1992). In developing countries, the demand for wheat is projected to increase by 60% (CIMMYT, 2017). As reported by Curtis (1992), intensifying the production of wheat to meet the growing demand can be done by expanding the area of wheat cultivation and enhancing the yield per unit sown. Additionally, reducing losses before and after harvest will allow more wheat available for consumption.

As at 2015, wheat accounted for 54% of French cereals and occupied about 4 million hectares (Ministère de l'Agriculture et de l'Alimentation, 2015). Oishmaya (2019), reported that the largest wheat producer in Europe is France (37 Mt) and the 5th globally. The greatest production is done in the north of the country and winter wheat is the main variety produced. Production is usually in the autumn season and harvested in August of the following year.

1.2.1 Impact of climate change in wheat production

Lopes et al. (2018), confirm that sporadic weather conditions associated with rising temperatures and rainfall cause specific challenges for wheat producers, and such patterns can also decrease improvements in the genetics of winter wheat. Several studies show the link between climate variabilities and wheat production. CIMMYT in 2017 reported that temperature increases as a result of climate change will cause a 20-30% decline in wheat production in developing countries. Although wheat can be grown in diverse environments, usually in countries where wheat is grown, grain filling occurs when temperatures are high and soil moisture is low (Asseng et al., 2009).

According to Gouache et al. (2012), several studies in France shown a negative relationship between rising temperatures and crop yields for wheat, maize, and barley (Lobell et al., 2011). In the study conducted by Xiao et al. (2018), the yield of wheat increased with an increase in carbon dioxide concentration, and Batts et al. (1998) also confirmed that wheat yield is very sensitive to carbon dioxide concentrations. The study conducted by Lopes et al. (2013) proved that optimal phenology is extremely associated with the temperature and rainfall at which genotypes of winter wheat were exposed during heading time; that is 20 days before and after heading. Currently, in France, heading dates occur earlier as a result of earlier stages of development due to increased temperatures (Gate et al., 2008). Similarly, in France, the study conducted by Brisson et al. (2010), shows that, during grain filling, high temperatures result in reduced wheat yields and due to climate change, in the future, heat stress will increase throughout grain filling (Gouache et al., 2012).

For control of these crises, some researchers have carried out studies to find solutions. Gouache et al. (2012), propose strategies like using improved cultivars (earlier heading cultivars) and modifying sowing dates. Also, phenology and heat stress focused breeding programs as studied by Olesen et al. (2011), have the potential to reduce the negative impact of climate change on wheat production.

1.3 Brown rust

Brown rust, also known as wheat leaf rust, is caused by the fungus *Puccinia triticina. P. triticina* belongs to the kingdom Fungi, phylum *Basidiomycota*, class *Urediniomycetes*, order *Uredinales*, family *Pucciniaceae* and genus *Puccinia* (Bolon et al., 2008). This fungus is a biotroph because of how it extracts nutrients from the cells of living hosts. It is also an obligate parasite because it needs a living organism for survival (Kolmer, 2013). To complete its life cycle, it requires two hosts, the main host (uredinial) and an alternate host (pycnial/aecial); making this fungus heteroecious. The main host is usually wheat and the alternate host is the meadow rue (Bolton et al., 2008). However, in France, the alternative host, Thalictrum speciosissimum, is not present and is very rare in Europe. At a global level, the absence of an alternative host and genotyping information for the mainstream wheat production zones indicate that the sexual phase is not involved in this disease's epidemiology, and is a marginal cause of genetic variation in the fungus (Bolton et al., 2008; Azzimonti, 2012). *P. triticina* reproduction is exclusively asexual in France, and segregates with the same phenotype are of the same SSR genotype, except for unusual mutations (Goyeau et al., 2007; Azzimonti, 2012). Brown rust can occur anywhere in the world where wheat is cultivated. The optimum conditions for its development are dewy environments, mild temperatures (15-25°C) usually during the flowering phase of hosts (Kolmer, 2017). *P. triticina* is an airborne pathogen that is slightly endocyclic (an organism with a low level of persistence), as opposed to highly endocyclic pests, as defined by Aubertot and Robin (2013).

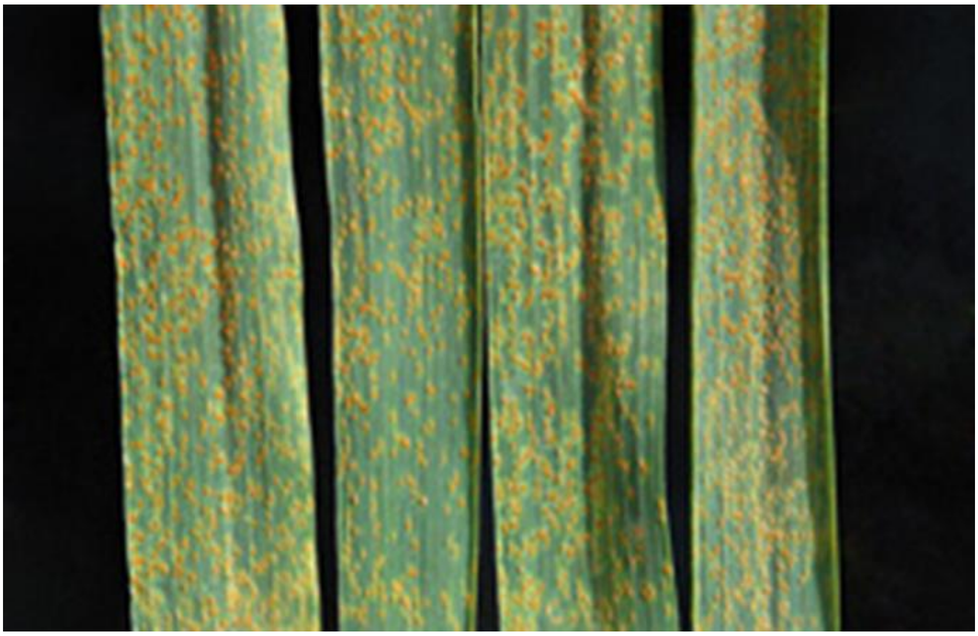

Figure 2: Close-up of leaf rust on wheat (Kolmer, 2006).

1.3.1 Life cycle, epidemiology, and symptom

According to Kolmer (2013), P. triticina has a complex life cycle in that; it grows on two unrelated hosts and has five different spore formation stages, namely; (i) on cereal hosts- teliospores, basidiospores, and urediniospores and (ii) on alternate hosts- pycniospores and aeciospores.

The rust develops when the asexual uredinial stage advances into sporulation under favourable conditions. When a crop is infected at an early stage, this disease can result in poor root and tiller formation, which subsequently results in a weak plant. In large cultivations, yield losses can range between 1-20%, whereas in favourable conditions, losses can be very devastating. In extreme cases, due to shrivelled grain and damaged tillers, losses can be up to 50% (Roelfs et al., 1992).

The symptom of *P. triticina* is characterised by brownish-orange and usually circular spots known as uredinia that appear on the upper surface of leaves. When infections are more severe, spots can also appear on sheaths. These spots can be dispersed by wind over long distances and constitute several spores (Robin et al., 2018). The establishment of the rust is usually a result of uredinia on volunteer plants that are transferred by the wind into fields causing severe infections on vulnerable crops. Germination occurs within 1-3 hours when the urediniospores get into contact with available moisture when there is a favourable temperature. The development of rust occurs when wind or rain transfer the urediniospores onto the surface of wheat leaves and these leaves absorb water or get into contact with moisture. These spores then swell up and form a germ tube usually after 4-8 hours under optimum conditions (Zhang et al., 2003; Bolton et al., 2008). The germ tube grows until it gets in touch with a stoma and produces an appressorium. According to Hirst and Hurst (1967), sometimes, during the transfer of the spores over long distances, these spores suspend in the air until they are cleared by rain. Although the spores are usually dispersed by wind, they can also be rain deposited.

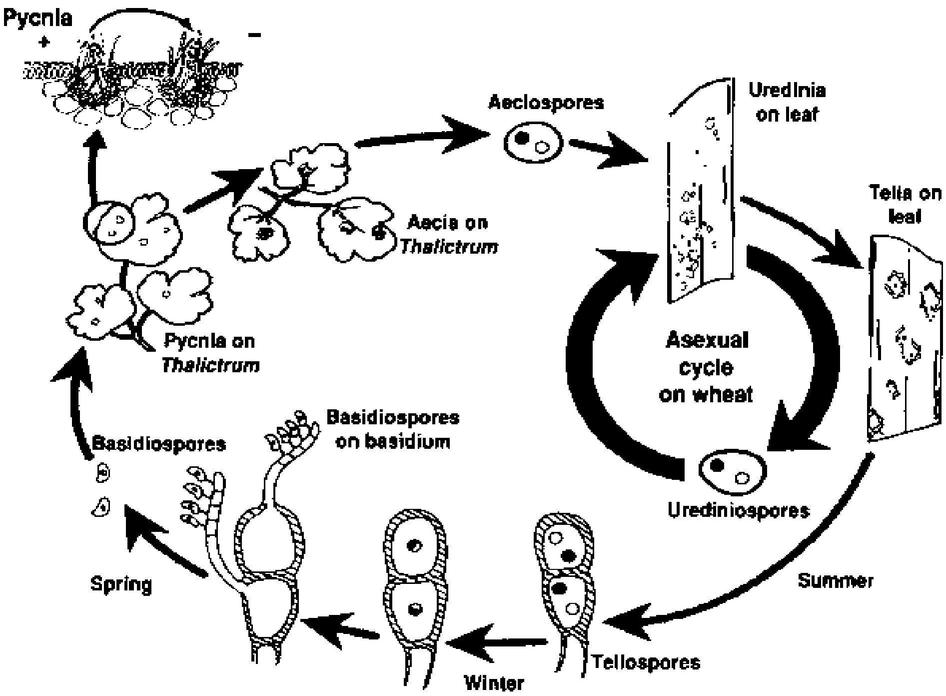

Figure 3: Life cycle of *Puccinia triticina* (Singh et al., 2002).

Table 1: Environmental conditions required for the development of wheat rust (Roelfs et al., 1992).

Stage	Temperature (°C)			Light	Free water
	Minimum	Optimum	Maximum		
Germination	2	20	30	Low	Essential
Germling	5	15-20	30	Low	Essential
Appressorium	-	15-20	-	None	Essential
Penetration	10	20	30	No effect	Essential
Growth	2	25	35	High	None
Sporulation	10	25	35	High	None

1.3.2 Brown rust in wheat production

A prominent disease of wheat is the brown rust, which causes adverse damages to wheat fields (Roelfs, 1992; Bolton et al., 2008). Worldwide, *P. triticina* is known to be a vital pathogen in wheat cultivation that causes substantial losses in cultivated areas (Kolmer, 2005). Yield losses can reach up to 70% in severe cases if not controlled (Robin et al., 2018), which results in reduced kernel biomass and kernel number per head. In past times, brown rust was not considered important as it caused less detrimental effects compared to other wheat diseases that affected grain quality (Leonard & Szabo, 2005; Bolton et al., 2008). According to Anikster et al. (2005), on wheat hosts, the urediniospores formed are dikaryotic and in the presence of leaf surface water and optimum temperature can re-infect the alternate host.

1.3.3 Control methods (impact of cropping practices notably)

The key approaches for leaf rust control depend on the use of cultivars with genetic resistance and the use of fungicides. Using resistant cultivars is the most desirable and most cost-effective method to reduce the effects of brown rust. Subsequently, Robin et al. (2018) describe the key control methods against brown rust as follows:

- Genetic resistance (mainly the use of resistant cultivar alone or in a cultivar mixture; Bolton et al., 2008; Goyeau and Lannou 2011).
- Fungicides application (Roelfs et al., 1992).
- Modify the status of the crop (balancing nitrogen fertilisation; sowing at appropriate rates; Robert et al., 2002; Robert et al., 2004).
- Escape strategy (sowing at a later date; Mishra et al., 1994) and
- Control of primary inoculum sources at field level by spatially distributing wheat fields and managing wheat volunteers; Anderson & Soper, 2003; Papaix et al., 2011).

1.3.4 Epidemiological models for brown rust in wheat

In the development of models for diseases, several methods can be used. Mechanistic models are developed based on theories, concepts, or hypotheses of how developments happen, and data gathered afterward can be used for improving the existing theories or concepts. Models established to describe observed phenomena or connection between variables using existing statistical ideologies are known as empirical models (El Jarroudi et al., 2018).

According to Nikolaev et al. (2019), due to the damages caused by brown rust in wheat, several tools have been developed to help monitor and predict its development as well as find measures for control. Most of these tools use several factors (biotic and abiotic) to critically assess the prevalence of brown rust (de Vallavieille-Pope et al., 2000). Other factors used may include meteorological factors and some epidemiological factors such as latent period, spore formation, infestation efficacy, and the ratio of developed lesions. Moreover, to properly develop these tools, an appropriate estimate of the growth of the pathogen must be ensured by comparing the ratio of developed lesions on a number of individuals (de Vallavieille-Pope et al., 2000). These models can be used to forecast infections under different weather conditions and future climates (Nikolaev et al., 2019). Some models used in predicting and controlling brown rust development are:

i. The RustDEp (Rust Development of Epidemics) model- a dynamic model for monitoring the daily progress of brown rust severity on wheat (Rossi et al., 1997).
ii. IPSIM-WHEAT model- a hierarchical, qualitative model used to predict the severity of brown rust as a function of cropping practices, climate, soil, and field environment (Robin & Aubertot, 2015).
iii. WHEATPEST model- A basic mechanistic winter wheat crop growth model that integrates damage mechanisms caused by multiple pests and simulates the physiological effects of these pests on plant growth and yield (Willocquet et al., 2008).
iv. STICS-MILA model- predicts significant variations in disease intensity between climatic periods and between scenarios (Caubel et al., 2017).

Appendix II: Analysis of warning bulletins

a. Example for Aquitaine 1985

YEAR/DAY/MONTH	REGION	BROWN RUST SEVERITY	REMARK	JUSTIFICATION
1985/28/Mar	AQUITAINE	1	First pustules observed.	
1985/4/Apr	AQUITAINE	1		The risk of brown rust gets worse with the hot weather.
1985/12/Apr	AQUITAINE	1	Only a few rare plots, sown before October 15-20 in Talent, Fidel, Gala and Hardi are affected by the Brown rust.	
1985/18/Apr	AQUITAINE	1		New outbreaks can be noted, mainly in the Dordogne, on Gala and Talent. It's still just first pustules on 1 leaves.
1985/24/Apr	AQUITAINE	1	A little change since last week and it is stagnant on the leaves.	
1985/3/May	AQUITAINE	2		This disease is currently evolving in the plots sown in varieties Talent, Fidel, Gala, Hardi, Frandoc, Castan and Festival.
1985/15/May	AQUITAINE	2	The disease is in notable progression on Talent varieties, Fidel, Gala, Hardi, Frandoc, Festival and Castan.	
1985/23/May	AQUITAINE	3		Rapid spread of the disease.

b. Example for Auvergne 1988

YEAR/DAY/MONTH	REGION	BROWN RUST SEVERITY	REMARK	JUSTIFICATION
1988/16/Mar	AUVERGNE	1	Brown Rust is already observed on susceptible varieties in many situations and in late October sowing.	
1988/7/Apr	AUVERGNE	1		Pustules on 1 leaves in some plots (sensitive varieties).
1988/21/Apr	AUVERGNE	1	Has not evolved since last bulletin.	
1988/17/May	AUVERGNE	1		S1 evolution; especially observed in the ALLIER. Pustules are rare in PUY-DE-DOME and HAUTE-LOIRE.
1988/31/May	AUVERGNE	2	Given the current cooler weather, moderate progress observed on the varieties: THESEE, FESTIVAL, TALENT, CAMP-REMY.	

Appendix III: Warning bulletins with varying weather indicators

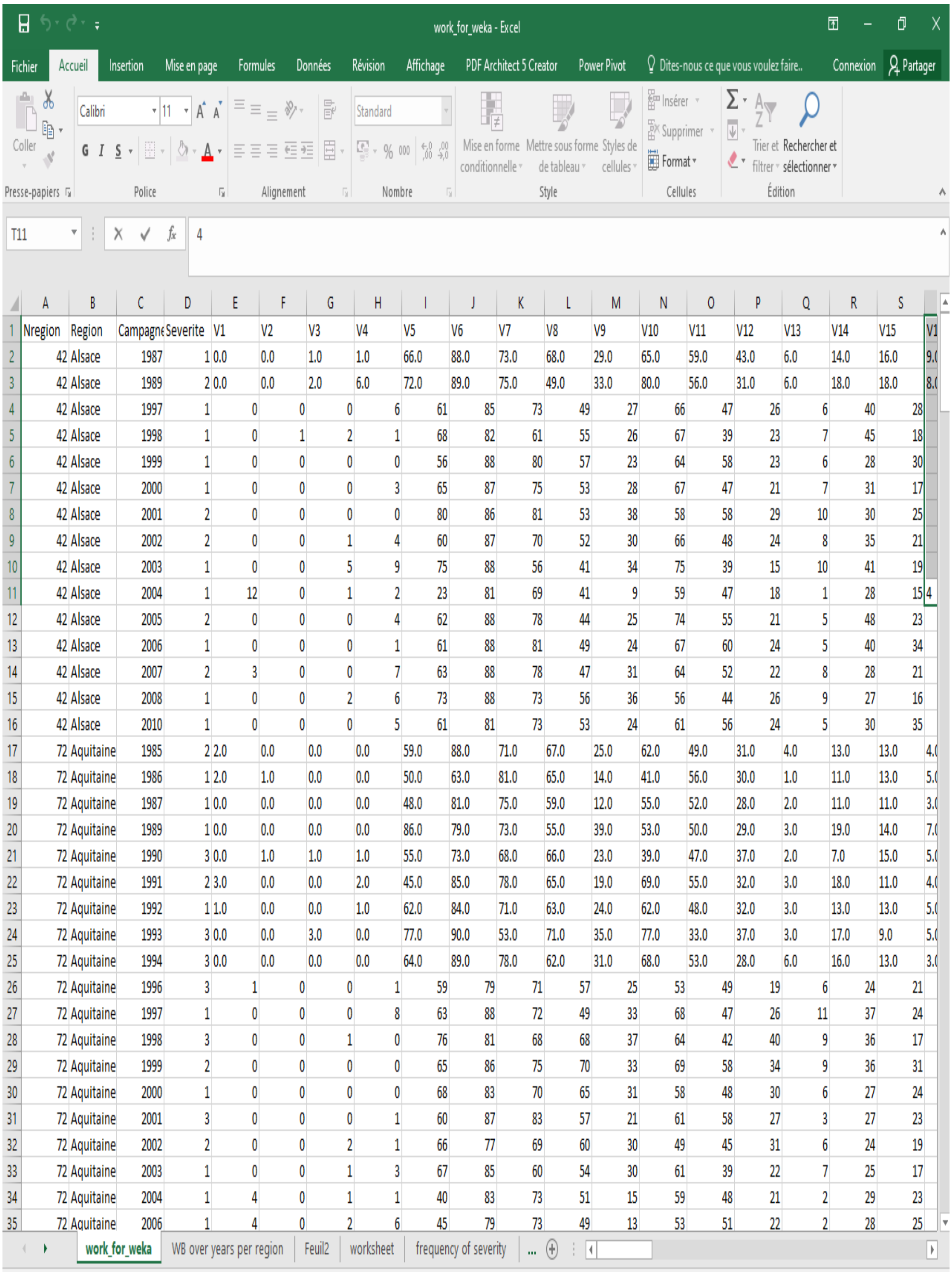

Nregion	Region	Campagne	Severite	V1	V2	V3	V4	V5	V6	V7	V8	V9	V10	V11	V12	V13	V14	V15	V1
42	Alsace	1987	1	0.0	0.0	1.0	1.0	66.0	88.0	73.0	68.0	29.0	65.0	59.0	43.0	6.0	14.0	16.0	9.(
42	Alsace	1989	2	0.0	0.0	2.0	6.0	72.0	89.0	75.0	49.0	33.0	80.0	56.0	31.0	6.0	18.0	18.0	8.(
42	Alsace	1997	1	0	0	0	6	61	85	73	49	27	66	47	26	6	40	28	
42	Alsace	1998	1	0	1	2	1	68	82	61	55	26	67	39	23	7	45	18	
42	Alsace	1999	1	0	0	0	0	56	88	80	57	23	64	58	23	6	28	30	
42	Alsace	2000	1	0	0	0	3	65	87	75	53	28	67	47	21	7	31	17	
42	Alsace	2001	2	0	0	0	0	80	86	81	53	38	58	58	29	10	30	25	
42	Alsace	2002	2	0	0	1	4	60	87	70	52	30	66	48	24	8	35	21	
42	Alsace	2003	1	0	0	5	9	75	88	56	41	34	75	39	15	10	41	19	
42	Alsace	2004	1	12	0	1	2	23	81	69	41	9	59	47	18	1	28	15	4
42	Alsace	2005	2	0	0	0	4	62	88	78	44	25	74	55	21	5	48	23	
42	Alsace	2006	1	0	0	0	1	61	88	81	49	24	67	60	24	5	40	34	
42	Alsace	2007	2	3	0	0	7	63	88	78	47	31	64	52	22	8	28	21	
42	Alsace	2008	1	0	0	2	6	73	88	73	56	36	56	44	26	9	27	16	
42	Alsace	2010	1	0	0	0	5	61	81	73	53	24	61	56	24	5	30	35	
72	Aquitaine	1985	2	2.0	0.0	0.0	0.0	59.0	88.0	71.0	67.0	25.0	62.0	49.0	31.0	4.0	13.0	13.0	4.(
72	Aquitaine	1986	1	2.0	1.0	0.0	0.0	50.0	63.0	81.0	65.0	14.0	41.0	56.0	30.0	1.0	11.0	13.0	5.(
72	Aquitaine	1987	1	0.0	0.0	0.0	0.0	48.0	81.0	75.0	59.0	12.0	55.0	52.0	28.0	2.0	11.0	11.0	3.(
72	Aquitaine	1989	1	0.0	0.0	0.0	0.0	86.0	79.0	73.0	55.0	39.0	53.0	50.0	29.0	3.0	19.0	14.0	7.(
72	Aquitaine	1990	3	0.0	1.0	1.0	1.0	55.0	73.0	68.0	66.0	23.0	39.0	47.0	37.0	2.0	7.0	15.0	5.(
72	Aquitaine	1991	2	3.0	0.0	0.0	2.0	45.0	85.0	78.0	65.0	19.0	69.0	55.0	32.0	3.0	18.0	11.0	4.(
72	Aquitaine	1992	1	1.0	0.0	0.0	1.0	62.0	84.0	71.0	63.0	24.0	62.0	48.0	32.0	3.0	13.0	13.0	5.(
72	Aquitaine	1993	3	0.0	0.0	3.0	0.0	77.0	90.0	53.0	71.0	35.0	77.0	33.0	37.0	3.0	17.0	9.0	5.(
72	Aquitaine	1994	3	0.0	0.0	0.0	0.0	64.0	89.0	78.0	62.0	31.0	68.0	53.0	28.0	6.0	16.0	13.0	3.(
72	Aquitaine	1996	3	1	0	0	1	59	79	71	57	25	53	49	19	6	24	21	
72	Aquitaine	1997	1	0	0	0	8	63	88	72	49	33	68	47	26	11	37	24	
72	Aquitaine	1998	3	0	0	1	0	76	81	68	68	37	64	42	40	9	36	17	
72	Aquitaine	1999	2	0	0	0	0	65	86	75	70	33	69	58	34	9	36	31	
72	Aquitaine	2000	1	0	0	0	0	68	83	70	65	31	58	48	30	6	27	24	
72	Aquitaine	2001	3	0	0	0	1	60	87	83	57	21	61	58	27	3	27	23	
72	Aquitaine	2002	2	0	0	2	1	66	77	69	60	30	49	45	31	6	24	19	
72	Aquitaine	2003	1	0	0	1	3	67	85	60	54	30	61	39	22	7	25	17	
72	Aquitaine	2004	1	4	0	1	1	40	83	73	51	15	59	48	21	2	29	23	
72	Aquitaine	2006	1	4	0	2	6	45	79	73	49	13	53	51	22	2	28	25	

Appendix IV: The detailed J48 pruned decision tree generated with WEKA.

```
Attributes:   109
=== Classifier model ===
J48 pruned tree
------------------
V63 <= 278.8
|   V81 <= 14.4
|   |   V69 <= 15.5: 1 (60.0/1.0)
|   |   V69 > 15.5
|   |   |   V7 <= 85.0
|   |   |   |   V21 <= 266.5
|   |   |   |   |   V15 <= 21.0
|   |   |   |   |   |   V70 <= 0.0
|   |   |   |   |   |   |   V80 <= 0.5
|   |   |   |   |   |   |   |   V38 <= 21.0
|   |   |   |   |   |   |   |   |   V72 <= 12.5
|   |   |   |   |   |   |   |   |   |   V38 <= 16.0
|   |   |   |   |   |   |   |   |   |   |   V36 <= 28.0: 1 (6.0)
|   |   |   |   |   |   |   |   |   |   |   V36 > 28.0
|   |   |   |   |   |   |   |   |   |   |   |   V28 <= 32.0: 1 (2.0)
|   |   |   |   |   |   |   |   |   |   |   |   V28 > 32.0: 2 (8.0)
|   |   |   |   |   |   |   |   |   |   V38 > 16.0: 1 (8.0)
|   |   |   |   |   |   |   |   |   V72 > 12.5: 2 (2.0/1.0)
|   |   |   |   |   |   |   |   V38 > 21.0
|   |   |   |   |   |   |   |   |   V16 <= 8.0: 2 (4.0)
|   |   |   |   |   |   |   |   |   V16 > 8.0: 3 (2.0)
|   |   |   |   |   |   |   V80 > 0.5: 1 (3.0/1.0)
|   |   |   |   |   |   V70 > 0.0: 1 (15.0/1.0)
|   |   |   |   |   V15 > 21.0: 1 (89.0/6.0)
|   |   |   |   V21 > 266.5
|   |   |   |   |   V2 <= 0.0
|   |   |   |   |   |   V68 <= 2.0
|   |   |   |   |   |   |   V72 <= 4.0: 1 (3.0)
|   |   |   |   |   |   |   V72 > 4.0
|   |   |   |   |   |   |   |   V13 <= 10.0
|   |   |   |   |   |   |   |   |   V5 <= 75.5: 2 (4.0)
|   |   |   |   |   |   |   |   |   V5 > 75.5: 3 (4.0)
|   |   |   |   |   |   |   |   V13 > 10.0
|   |   |   |   |   |   |   |   |   V6 <= 86.5: 1 (2.0)
|   |   |   |   |   |   |   |   |   V6 > 86.5
|   |   |   |   |   |   |   |   |   |   V25 <= 31.0: 1 (2.0)
|   |   |   |   |   |   |   |   |   |   V25 > 31.0: 2 (7.0)
|   |   |   |   |   |   V68 > 2.0: 1 (2.0)
|   |   |   |   |   V2 > 0.0
|   |   |   |   |   |   V4 <= 1.0: 3 (2.0)
|   |   |   |   |   |   V4 > 1.0: 1 (2.0)
|   |   |   V7 > 85.0: 2 (6.0/1.0)
|   V81 > 14.4
|   |   V48 <= 62.0
|   |   |   V72 <= 17.0: 1 (10.0)
|   |   |   V72 > 17.0
|   |   |   |   V55 <= 3.0
|   |   |   |   |   V16 <= 6.0: 1 (6.0/1.0)
|   |   |   |   |   V16 > 6.0: 2 (4.0)
|   |   |   |   V55 > 3.0
|   |   |   |   |   V99 <= 6.6: 2 (5.0)
|   |   |   |   |   V99 > 6.6: 3 (3.0)
|   |   V48 > 62.0
|   |   |   V6 <= 83.0: 1 (2.0)
|   |   |   V6 > 83.0: 3 (9.0)
V63 > 278.8
|   V77 <= 0.5: 1 (2.0)
|   V77 > 0.5
|   |   V86 <= 5.6
|   |   |   V2 <= 1.0
|   |   |   |   V12 <= 46.0: 3 (12.0)
|   |   |   |   V12 > 46.0: 2 (2.0)
|   |   |   V2 > 1.0: 2 (4.0)
|   |   V86 > 5.6
|   |   |   V6 <= 87.0: 2 (9.0)
|   |   |   V6 > 87.0: 1 (3.0/1.0)
Number of Leaves  :     34
Size of the tree :      67
```

Appendix V: Model attributes of the decision tree and their meanings.

ATTRIBUTE	MEANING
V1	med,j,hr,inf50,t3- median of the number of days when relative humidity is below 50% during the 3rd trimester.
V2	med,j,hr,inf50,t4- median of the number of days when relative humidity is below 50% during the 4th trimester.
V3	med,j,hr,inf50,t1- median of the number of days when relative humidity is below 50% during the 1st trimester.
V4	med,j,hr,inf50,t2- median of the number of days when relative humidity is below 50% during the 2nd trimester.
V5	med,j,hr,sup70,t3- median of the number of days when relative humidity is above 70% during the 3rd trimester.
V6	med,j,hr,sup70,t4- median of the number of days when relative humidity is above 70% during the 4th trimester.
V7	med,j,hr,sup70,t1- median of the number of days when relative humidity is above 70% during the 1st trimester.
V8	med,j,hr,sup70,t2- median of the number of days when relative humidity is above 70% during the 2nd trimester.
V9	med,j,hr,sup80,t3- median of the number of days when relative humidity is above 80% during the 3rd trimester
V10	med,j,hr,sup80,t4- median of the number of days when relative humidity is above 80% during the 4th trimester.
V11	med,j,hr,sup80,t1- median of the number of days when relative humidity is above 80% during the 1st trimester.
V12	med,j,hr,sup80,t2- median of the number of days when relative humidity is above 80% during the 2nd trimester.
V13	med,j,hr,sup90,t3- median of the number of days when relative humidity is above 90% during the 3rd trimester.
V14	med,j,hr,sup90,t4- median of the number of days when relative humidity is above 90% during the 4th trimester.
V15	med,j,hr,sup90,t1- median of the number of days when relative humidity is above 90% during the 1st trimester.
V16	med,j,hr,sup90,t2- median of the number of days when relative humidity is above 90% during the 2nd trimester.
V17	med,cum,hr,t3- median of the cumulative relative humidity during the 3rd trimester.
V18	med,cum,hr,t4- median of the cumulative relative humidity during the 4th trimester.
V19	med,cum,hr,t1- median of the cumulative relative humidity during the 1st trimester.
V20	med,cum,hr,t2- median of the cumulative relative humidity during the 2nd trimester.
V21	med,cum,p,t3- median of the cumulative rainfall during the 3rd trimester.
V22	med,cum,p,t4- median of the cumulative rainfall during the 4th trimester.
V23	med,cum,p,t1- median of the cumulative rainfall during the 1st trimester.
V24	med,cum,p,t2- median of the cumulative rainfall during the 2nd trimester.
V25	med,j,sans,p,t3- median of the number of days without rainfall during the 3rd trimester.
V26	med,j,sans,p,t4- median of the number of days without rainfall during the 4th trimester.
V27	med,j,sans,p,t1- median of the number of days without rainfall during the 2nd trimester.
V28	med,j,sans,p,t2- median of the number of days without rainfall during the 1st trimester.
V29	med,j,avec,p,t3- median of the number of days with rainfall during the 3rd trimester.
V30	med,j,avec,p,t4- median of the number of days with rainfall during the 4th trimester.
V31	med,j,avec,p,t1- median of the number of days with rainfall during the 1st trimester.
V32	med,j,avec,p,t2- median of the number of days with rainfall during the 2nd trimester.
V33	med,j,p,sup2,t3- median of the number of days with rainfall above 2mm during the 3rd trimester.
V34	med,j,p,sup2,t4- median of the number of days with rainfall above 2mm during the 4th trimester.
V35	med,j,p,sup2,t1- median of the number of days with rainfall above 2mm during the 1st trimester.
V36	med,j,p,sup2,t2- median of the number of days with rainfall above 2mm during the 2nd trimester.
V37	med,j,p,sup5,t3- median of the number of days with rainfall above 5mm during the 3rd trimester.
V38	med,j,p,sup5,t4- median of the number of days with rainfall above 5mm during the 4th trimester.
V39	med,j,p,sup5,t1- median of the number of days with rainfall above 5mm during the 1st trimester.
V40	med,j,p,sup5,t2- median of the number of days with rainfall above 5mm during the 2nd trimester.
V41	med,cum,rg,t3- median of the cumulative global radiation during the 3rd trimester.
V42	med,cum,rg,t4- median of the cumulative global radiation during the 4th trimester.
V43	med,cum,rg,t1- median of the cumulative global radiation during the 1st trimester.
V44	med,cum,rg,t2- median of the cumulative global radiation during the 2nd trimester.
V45	med,sin,tm5<25,t3- median of the temporal integration during t3of the sin^2 function (0 when temp is below 5°C or above 25°C)
V46	med,sin,tm5<25,t4- median of the temporal integration during t4 of the sin^2 function (0 when temp is below 5°C or above 25°C)
V47	med,sin,tm5<25,t1- median of the temporal integration during t1of the sin^2 function (0 when temp is below 5°C or above 25°C)
V48	med,sin,tm5<25,t2- median of the temporal integration during t2 of the sin^2 function (0 when temp is below 5°C or above 25°C)
V49	med,sin,tm5<25,hr80,t3- median of the temporal integration during t3 of the sin^2 function (0 when temp is <5°C or >25°C, or RH <80%)
V50	med,sin,tm5<25,hr80,t4- median of the temporal integration during t4 of the sin^2 function (0 when temp is <5° C or >25°C, or RH <80%)
V51	med,sin,tm5<25,hr80,t1- median of the temporal integration during t1 of the sin2 function (0 when temp is <5° C or >25°C, or RH <80%)
V52	med,sin,tm5<25,hr80,t2- median of the temporal integration during t2 of the sin2 function (0 when temp is <5° Cor >25°C, or RH <80%)
V53	med,j,tm,inf0,t3- median of the number of days with temp below 0°C in t3
V54	med,j,tm,inf0,t4- median of the number of days with temp below 0°C in t4
V55	med,j,tm,inf0,t1- median of the number of days with temp below 0°C in t1
V56	med,j,tm,inf0,t2- median of the number of days with temp below 0°C in t2
V57	med,j,tn,inf0,t3- median of the number of days with tmin below 0°C in t3
V58	med,j,tn,inf0,t4- median of the number of days with tmin below 0°C in t4
V59	med,j,tn,inf0,t1- median of the number of days with tmin below 0°C in t1
V60	med,j,tn,inf0,t2- median of the number of days with tmin below 0°C in t2
V61	med,tp,ther5,t3- median of the thermal time (5°C) during t3
V62	med,tp,ther5,t4- median of the thermal time (5°C) during t4
V63	med,tp,ther5,t1- median of the thermal time (5°C) during t1
V64	med,tp,ther5,t2- median of the thermal time (5°C) during t2
V65	med,j,tm,sup25,t3- median of the number of days with temp above 25°C in t3
V66	med,j,tm,sup25,t4- median of the number of days with temp above 25°C in t4
V67	med,j,tm,sup25,t1- median of the number of days with temp above 25°C in t1
V68	med,j,tm,sup25,t2- median of the number of days with temp above 25°C in t2
V69	med,j,tx,sup25,t3- median of the number of days with tmax above 25°C in t3
V70	med,j,tx,sup25,t4- median of the number of days with tmax above 25°C in t4
V71	med,j,tx,sup25,t1- median of the number of days with tmax above 25°C in t1
V72	med,j,tx,sup25,t2- median of the number of days with tmax above 25°C in t2
V73	med,j,tm,sup32,t3- median of the number of days with temp above 32°C in t3
V74	med,j,tm,sup32,t4- median of the number of days with temp above 32°C in t4
V75	med,j,tm,sup32,t1- median of the number of days with temp above 32°C in t1
V76	med,j,tm,sup32,t2- median of the number of days with temp above 32°C in t2
V77	med,j,tx,sup32,t3- median of the number of days with tmax above 32°C in t3
V78	med,j,tx,sup32,t4- median of the number of days with tmax above 32°C in t4
V79	med,j,tx,sup32,t1- median of the number of days with tmax above 32°C in t1
V80	med,j,tx,sup32,t2- median of the number of days with tmax above 32°C in t2
V81	med,moy,tn,t3- median of daily average minimum temperatures in t3
V82	med,moy,tn,t4- median of daily average minimum temperatures in t4
V83	med,moy,tn,t1- median of daily average minimum temperatures in t1
V84	med,moy,tn,t2- median of daily average minimum temperatures in t2
V85	med,tn,t3- median of minimum temperatures in t3
V86	med,tn,t4- median of minimum temperatures in t4
V87	med,tn,t1- median of minimum temperatures in t1
V88	med,tn,t2- median of minimum temperatures in t3
V89	med,moy,tx,t3- median of daily average maximum temperatures in t3
V90	med,moy,tx,t4- median of daily average maximum temperatures in t4
V91	med,moy,tx,t1- median of daily average maximum temperatures in t1
V92	med,moy,tx,t2- median of daily average maximum temperatures in t32
V93	med,tx,t3- median of maximum temperatures in t3
V94	med,tx,t4- median of maximum temperatures in t4
V95	med,tx,t1- median of maximum temperatures in t1
V96	med,tx,t2- median of maximum temperatures in t2
V97	med,moy,tm,t3- median of daily average temperatures in t3
V98	med,moy,tm,t4- median of daily average temperatures in t4
V99	med,moy,tm,t1- median of daily average temperatures in t1
V100	med,moy,tm,t2- median of daily average temperatures in t2
V101	med,3j,tm,sup25,dis,t3- median of number of dissociated sequences of 3 consecutive days with temp above 25°C in t3
V102	med,3j,tm,sup25,dis,t4- median of number of dissociated sequences of 3 consecutive days with temp above 25°C in t4
V103	med,3j,tm,sup25,dis,t1- median of number of dissociated sequences of 3 consecutive days with temp above 25°C in t1
V104	med,3j,tm,sup25,dis,t2- median of number of dissociated sequences of 3 consecutive days with temp above 25°C in t2
V105	med,3j,tm,sup25,nd,t3- median of number of non-dissociated sequences of 3 consecutive days with temp above 25°C in t3
V106	med,3j,tm,sup25,nd,t4- median of number of non-dissociated sequences of 3 consecutive days with temp above 25°C in t4
V107	med,3j,tm,sup25,nd,t1- median of number of non-dissociated sequences of 3 consecutive days with temp above 25°C in t1
V108	med,3j,tm,sup25,nd,t2- median of number of non-dissociated sequences of 3 consecutive days with temp above 25°C in t2

Appendix VI: R scripts used for RUE calculation

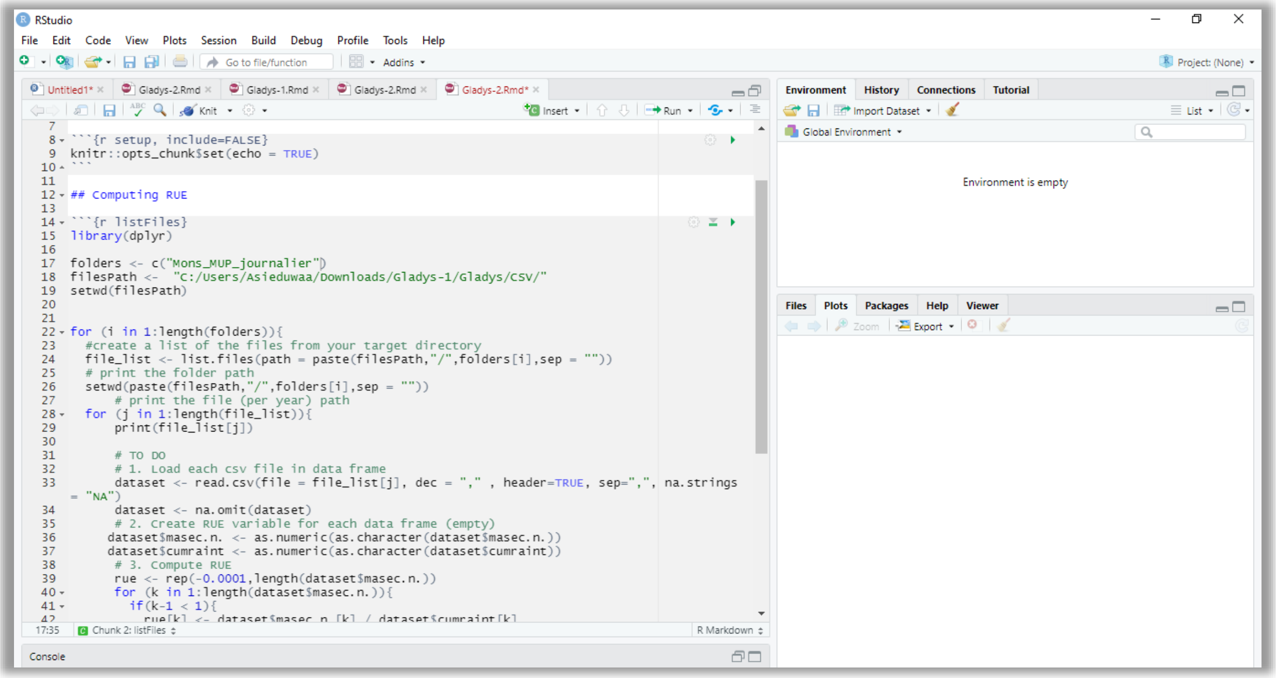

Norges miljø- og biovitenskapelige universitet
Noregs miljø- og biovitskapelege universitet
Norwegian University of Life Sciences

Postboks 5003
NO-1432 Ås
Norway